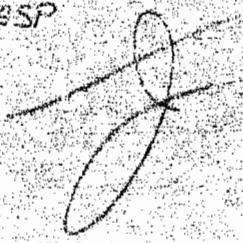


TIGHT GAS SANDS LIBRARY - WBSP

SAND78-1578

UNLIMITED RELEASE

DATA BASE 217



# HYDRAULIC FRACTURE BEHAVIOR AT A GEOLOGIC FORMATION INTERFACE: PRE-MINEBACK REPORT

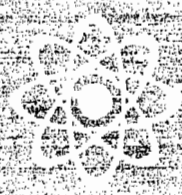
N. R. WARPINSKI, R. A. SCHMIDT  
D. A. NORTHROP, AND L. D. TYLER

Prepared by Sandia Laboratories, 2700 University Ave., Albuquerque, New Mexico 87123  
and Livermore, California 94550 for the United States Department of Energy under Contract AT(29-1)11789

PRINTED OCTOBER 1978



Sandia Laboratories  
Energy Research



SAND78-1578  
Unlimited Release

HYDRAULIC FRACTURE BEHAVIOR AT A GEOLOGIC FORMATION

INTERFACE: PRE-MINEBACK REPORT\*

by

N. R. Warpinski, R. A. Schmidt, D. A. Northrop,

Geotechnology Research Division

and

L. D. Tyler

Geological Projects Division

Sandia Laboratories

Albuquerque, NM 87185

ABSTRACT

An experiment has been conducted to study hydraulic fracture behavior at a geologic formation interface. Fractures were initiated above and below an interface between welded tuff with modulus of elasticity ( $E$ ), Poisson's ratio ( $\nu$ ), porosity ( $\phi$ ) and permeability ( $k$ ) of  $3.8 \times 10^6$  psi, 0.239, 13% and 0.01 md, respectively, overlying a bedded ash-fall tuff with  $E$ ,  $\nu$ ,  $\phi$ , and  $k$  of  $2.4 \times 10^5$  psi, 0.312, 45% and 0.01 md, respectively. Nine-thousand gallons and five thousand gallons of colored cement were injected into the ash-fall tuff and welded tuff, respectively, at a flow rate of 6 bbl/min. Conventional fracture design calculations indicated that this volume was sufficient to propagate 50 ft high fractures, 600 ft total length in each zone. Material property measurements from logs and laboratory tests on core samples, in situ stresses in adjacent regions, design calculations, pumping schedules and treatment operations relevant to this experiment are described. Mineback through the experiment regions has been initiated and will allow direct observation of the created fracture systems. Evaluation of the fracture behavior, particularly at the interface, will be performed during mineback and integrated with the present data to provide a better understanding of hydraulic fracturing.

\*This work was supported by the U. S. Department of Energy (DOE) under contract number AT(29-1)789.

TABLE OF CONTENTS

	Page
I. Introduction .....	2
II. Fracture Behavior at a Formation Interface .....	3
III. Geology of the U12g Tunnel Area .....	5
IV. Material Properties .....	9
V. In Situ Stresses .....	12
VI. Fracture Design .....	14
VII. Experimental Operations .....	27
Zone #1 - Ash-Fall Tuff .....	28
Zone #2 - Welded Tuff .....	30
VIII. Results and Discussion .....	33
SUMMARY .....	40
ACKNOWLEDGMENTS .....	40
REFERENCES .....	40

NOTE ADDED PRIOR TO PUBLICATION

Initial evaluation of this experiment has been made by mining along the interface. Preliminary observations include: (1) the first (lower) fracture easily penetrated the interface and broke upwards into a formation of significantly higher modulus; (2) fracture length was 150 ft (vs. 600 ft design) at the elevation of the interface; (3) the second (upper) fracture initiated in the same plane as the first fracture and propagated along it at several locations; (4) natural fractures in the welded tuff affected fracture behavior; (5) fracture widths were consistent with properties and design, 5-10 mm and 2-5 mm in the ash-fall and welded tuffs, respectively, and (6) observed fracture orientation was the same as the azimuth determined by seismic instrumentation. These results are preliminary; further information will be given in subsequent project publications and a final report for this experiment.

## I. INTRODUCTION

The generally non-economic gas production that is often obtained from massive hydraulic, dendritic, foam, gas, and chemical explosive fracturing has usually been attributed to either inadequate reservoir characterization or unfavorable and unexpected fracture behavior. The latter result includes many different possible phenomena, none of which are readily observed from the well bore. In situ examination of hydraulic fractures through mineback techniques, however, offers an ideal method of conducting fracture research and observing firsthand the effects of faults, fractures, geologic interfaces, and variations in in situ stresses, elastic moduli, and other important parameters. Such observations, together with complete pumping schedules, pressure records, geologic structure, material properties and in situ stress measurements, should be sufficient to characterize the fracture, compare the end result with that predicted by models and hopefully offer insight into the phenomena of fracture propagation.

U12g tunnel in Rainier Mesa at the Nevada Test Site has provided a site for in situ observations of hydraulic fractures through mineback as an ongoing experimental program relating to nuclear containment studies. Recently, DOE's Enhanced Gas Recovery Program funded a project to utilize this unique laboratory to understand and improve fracture technology and theory. Results of several previous experiments have been reported.<sup>1-5</sup>

The behavior of a hydraulic fracture at a formation interface is important in stimulation of a natural gas reservoir. A hydraulic fracture is usually designed to be contained within the pay zone where it was initiated. Failure to do this results in an effective loss of the expensive fluid and proppant used to fracture the unproductive strata or other deleterious effects should the fracture penetrate a water-bearing zone. Present design calculations assume that the hydraulic fracture is bounded and this results in a vertical, wedge-shaped fracture of constant height. Initially, it was hypothesized that the thickness of the boundary shale strata controlled vertical fracture growth.<sup>6</sup> It was recognized, however, that the mechanical properties of the different reservoir rocks and the in situ stresses would influence the shape of the hydraulic fracture.<sup>6-8</sup> Present understanding does not allow prediction of hydraulic fracture behavior at a formation interface.

A joint working group, consisting of Halliburton, Dowell, Amoco, and Sandia representatives, convened in Tulsa, Oklahoma, in February, 1977, to initiate planning of a "Formation Interface Experiment". Subsequent fracture design meetings were held with Dowell in March and July, 1977. The experiment was designed to test fracture growth both above and below a geologic formation consisting of a bedded ash-fall

tuff overlain by a welded ash-flow tuff. The subsequent interaction of the fractures with the interface would then be studied and mapped through mineback techniques. Two hydraulic fracture experiments were conducted in August and October, 1977.

This report presents all the data obtained to date for the experiments prior to mineback and evaluation. It contains geologic site information, formation material properties, fracture design calculations, and field data collected during the two fracture operations. Observations, predictions and conclusions concerning the behavior of the fracture are offered wherever possible. Combined with subsequent results from the mineback evaluation, this study will aid in the understanding of the mechanics of hydraulic fracturing.

## II. FRACTURE BEHAVIOR AT A FORMATION INTERFACE

Studies to date have investigated the properties and conditions of the different strata and the interface between them. Daneshy<sup>9</sup> investigated the strength of the interface in laboratory fracturing experiments and found that a fracture would propagate across a well-bonded interface between dissimilar rocks, but a weak interface, or an unbonded one, would arrest crack growth. An excellent example is the fracture termination at a "clean", weak coal seam - shale interface observed during fracturing to promote methane drainage of the seam prior to mining.<sup>10</sup> Hanson et al<sup>11</sup> have recently found that the stress perpendicular to an unbonded interface between blocks of the same material affects fracture penetration; presumably the roughness of the surfaces and the frictional effect of the applied stress are determining factors. However, they also noted that dynamic effects may also play a role since their results were dependent upon the pressure at which the crack initiated and grew. Simonson et al<sup>12</sup> and Rogers et al<sup>13</sup> have examined the rock mechanics aspects of hydraulic fracture containment. Specifically, they conclude that: (1) a fracture will tend not to penetrate into a bounding layer if the modulus of this layer is greater than the pay zone, (2) greater values of the minimum horizontal in situ stress in the bounding layers tend to inhibit the vertical extension of fractures, and (3) the relative gradients of the hydraulic fluid density and of the minimum horizontal in situ stress influence the upwards or downwards growth of the fracture.

Many problems dealing with fracture propagation in brittle materials have been analyzed using the concepts of linear elastic fracture mechanics. The success of this approach lies in the fact that in a single isotropic material the entire stress field near a crack tip can be described by a single parameter,  $K$ , known as the stress intensity factor.\* Since the mechanisms that govern fracture propagation behavior occur

\*This discussion deals only with the opening mode, or mode I, of crack growth.

occur near the crack tip, it is easy to understand why  $K$  is the parameter that governs crack growth. The fracture criterion is simply that crack growth will occur when  $K$  reaches a critical value,  $K_c$ . Since  $K$  depends on the loading and crack geometry, this criterion means that a certain combination of load and crack size is required to cause crack growth.

The simplicity of a single parameter description of the crack tip stress field is lost when one considers a crack whose tip rests at a material interface. If the elastic moduli of the materials on either side of the interface differ, then the description of the stress field requires two parameters. This situation is likely to require a more complex fracture criterion.

Many stress analyses have been performed on the problem of a crack approaching, reaching and passing through a material interface.<sup>14-18</sup> The stress analysis, however, is only half the answer since without a fracture criterion one cannot predict when the crack will grow. The most obvious approach is to ignore the case of a crack whose tip rests at the interface, examine the value of  $K$  as the crack tip approaches the interface, and assume that crack growth simply requires a value of  $K$  equal to  $K_c$ .<sup>12,14</sup> This simplified approach leads directly to the prediction that a crack will be arrested in one material and will not even reach the interface if the second material has a higher modulus than the first. This results from the fact that for even a slight modulus increase, the stress intensity factor goes to zero as the crack tip approaches the interface. Conversely, if the second material is of lower modulus than the first, the prediction is that crack growth will be enhanced and the crack will traverse the interface rapidly. Obviously, the problem has been oversimplified since much experimental evidence, particularly for composite materials, refutes these predictions.

One potential source of difficulty is in modeling the interface as a discontinuity. The interfaces in hydraulic fracture containment problems and the present experiment are not discrete. Instead, the change in modulus is observed to occur over some finite distance. If the interface were "smeared" in the stress analysis it might be possible to avoid the situation by which  $K$  approaches zero as the interface is approached. Some analytical work by Atkinson<sup>19</sup> deals with the subject of stress analysis for a crack in a medium with a continuously varying modulus, but his work deals with mode III and a modulus variation inappropriate for our needs. It may be possible to perform the necessary calculations using a finite element code (e.g., CHILES<sup>20</sup>) by assuming the proper form of stress singularity and using several discrete material layers of increasing modulus to smear the

interface artificially. These approaches might give more realistic predictions and would still allow for the use of the simple fracture criterion of  $K = K_c$ . Analytical and numerical calculations along these lines have been initiated.

An important parameter in hydraulic fracture containment is the variation in the minimum principal stress.<sup>12</sup> Unfortunately, rough calculations show that crack growth may be so sensitive to the value of the minimum principal stress that this variation can't be determined with enough accuracy with present technology to allow for accurate prediction.

The essence, then, is the realization of the inconsistencies observed in the behavior of fractures as seen in fracture mechanics analyses, laboratory experiments and the field. Examination of the present formation interface experiment in light of this experience does not allow a quantitative prediction of fracture behavior. In fact, disparate conditions exist: "well-bonded" interfaces with an order of magnitude range in the moduli. Thus, improvements in existing theories are required and will be an integral part of this program. At this stage, it is felt that more realistic modeling of the actual interfaces as seen in the field is the improvement with the most promising return.

### III. GEOLOGY OF THE U12g TUNNEL AREA

U12g tunnel is one of a number of tunnels that have been driven into Rainier Mesa for the purpose of conducting underground nuclear tests. The location of Rainier Mesa within the Nevada Test Site (NTS) is shown in Fig. 1. The geologic formations underlying Rainier Mesa are of volcanic origin resulting from activity throughout the Tertiary Period. In the vicinity of U12g tunnel, the sequence of volcanic beds has been divided into four major geologic units.<sup>21</sup> In the descending order, these are the Timber Mountain Tuff, Paintbrush Tuff, Belted Range Tuff, and Indian Trail Formation as shown in Fig. 2.

The Timber Mountain Tuff, which varies in thickness from about 150 ft to 450 ft in Rainier Mesa, is composed of the Ammonia Tanks Member, which is nearly entirely eroded off the top of the mesa, and the Rainier Mesa Member, which is vitric, very densely welded unit overlying a basal nonwelded tuff. The upper, densely welded unit of the Rainier Mesa Member is the effective cap rock of the mesa.

The Paintbrush Tuff (600-900 feet) is, in general, comprised of the Tiva Canyon, Pah Canyon, Topopah Spring, and Stockade Wash Members and unnamed bedded tuffs. Near U12g tunnel, however, only the Tiva Canyon Member, which is a partly welded ash-flow tuff, and the Stockade Wash Member, which is zeolitized ash-flow tuff, are observed.

The Belted Range Tuff in the vicinity of U12g tunnel consists of the Grouse Canyon Member which is a gray to reddish welded tuff with a thickness varying from

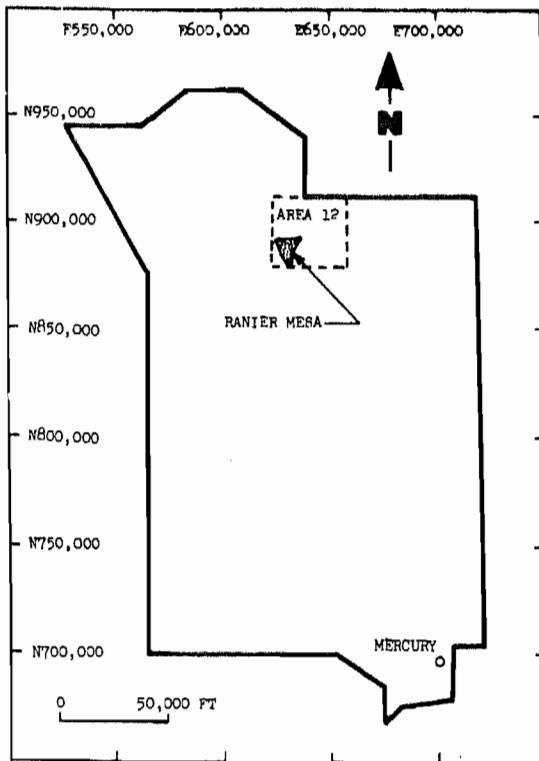


Figure 1. Nevada Test Site and Ranier Mesa.

TERTIARY	PLIOCENE	TIMBER MOUNTAIN TUFF	AMMONIA TANKS MBR
			RANIER MESA MBR
		PAINTBRUSH TUFF	BEDDED TUFF
			TIVA CANYON MBR
			BEDDED TUFF
			STOCKADE WASH MBR
	MIOCENE	BELTED RANGE TUFF	BEDDED TUFF
			GROUSE CANYON MBR
		INDIAN TRAIL FORMATION	TUNNEL BED 5
			TUNNEL BED 4
			TUNNEL BED 3
			TUNNEL BED 2
TUNNEL BED 1			

Figure 2. Stratigraphic Nomenclature Chart.

0 to ~100 feet. The Indian Trail Formation is composed of the Tunnel Beds, units 1-5. The Tunnel Bed, unit 5, is a well layered peralkaline ash-fall tuff (~100 feet), and the Tunnel Beds, units 1-4, are also well layered ash-fall tuffs of gray to pinkish brown color. Both Tunnel Bed 4 and 5 are zeolitized.

As shown in the geologic cross section in Fig. 3, the U12g tunnel complex was driven in the Tunnel Beds, units 2, 3, 4, and 5. The portal, which was driven into the base of the mesa escarpment, is at an elevation of 6114 ft, and the crest of the mesa rises to 7600 feet, providing an effective maximum overburden stress of 1000 to 1400 psi. The layout of the entire U12g complex is shown in Fig. 4. The bedded tuffs are excellent media in which to conduct fracture studies because of their uniformity of physical characteristics and absence of zones of native fracturing. Faults are present, but are typically of small displacement and rehealed. Hydraulic fracture tests have been performed near the Number 10 drift of U12g (U12g.10) from wells drilled from the top of the mesa and identified in Figs. 4 and 5 as UE12g10#3, UE12g10#5, and the present test UE12g10#6. Overcores of hydraulic fracture breakdown tests for in situ stress measurements have been conducted at the designated (HFS) locations<sup>1,22</sup> shown in Fig. 4.





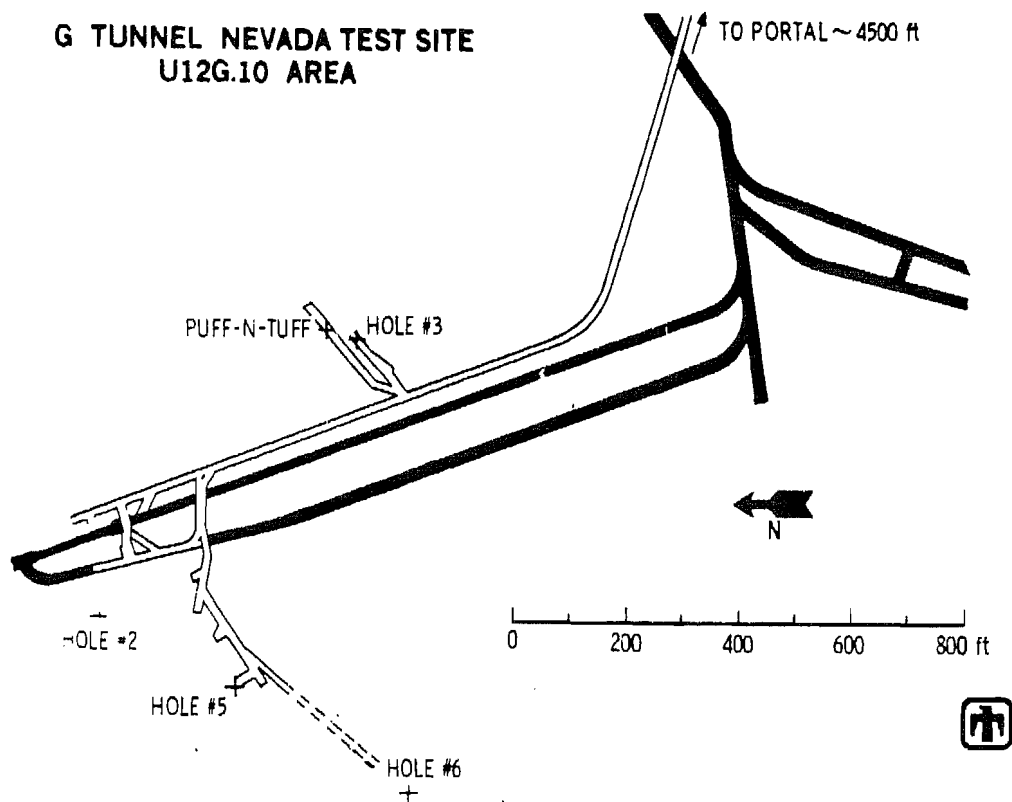


Figure 5. U12g.10 Experiments.

The interface experiment made use of the contact between the Tunnel Beds, unit 5, and the overlying Grouse Canyon Member. This contact is at a depth of 1348 feet (el. 6207), about 40 feet above tunnel level, and can be easily seen from the density log in Fig. 6. The welded tuff is considerably denser than the surrounding ash-fall tuffs. The electric log shown in Fig. 7 is also useful in determining the location and contacts of a welded tuff, since the resistivity increases with degree of welding.<sup>23</sup> The welded tuff lies from 1300 feet to 1348 feet with the densest section from 1320 feet to 1336 feet. Above and below the dense section are transition regions containing voids, fractures and breccia.

#### IV. MATERIAL PROPERTIES

The ash-fall tuffs are, in general, an excellent medium for conducting fracture research because of their uniformity; however, variations in grain size, bedding planes, geologic alteration and other factors do affect the material properties. The ash-flow tuffs exhibit no such uniformity as would be expected from their depositional history. Typical ash flow units have rock types ranging from very densely welded zones to extremely porous, brecciated, non-welded zones. Material

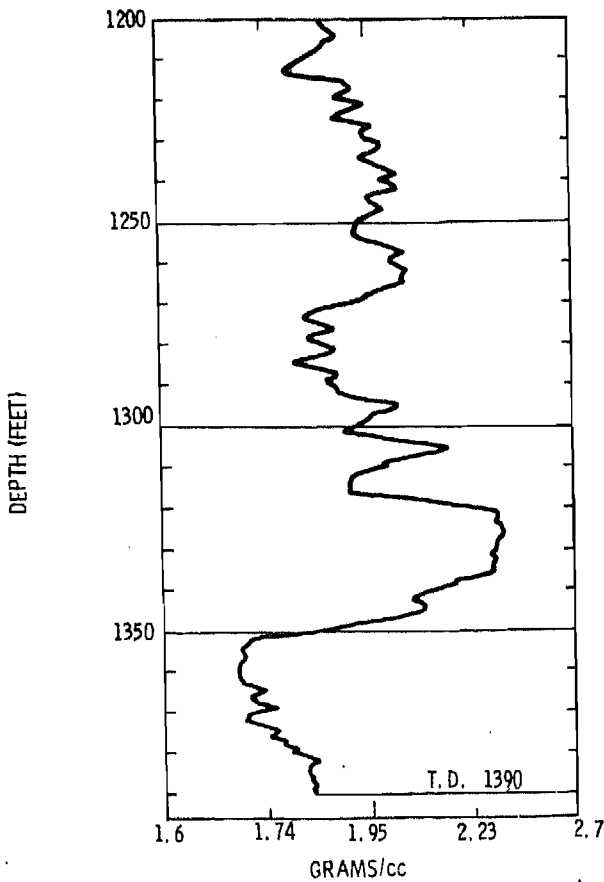


Figure 6. Density Log of UEL2g10#6.

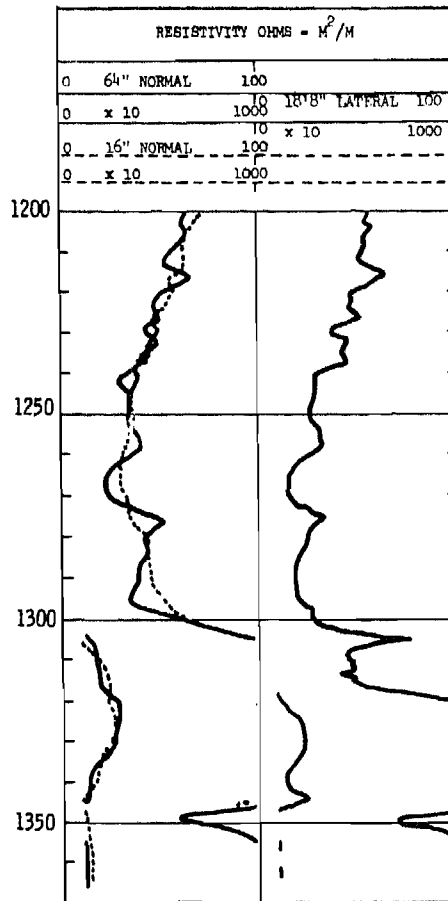


Figure 7. Resistivity Log of UEL2g10#6.

property measurements have been obtained in order to quantify the variations in these materials.

Material property measurements were obtained from eight core samples of the Grouse Canyon ash-flow tuff unit and the underlying per-alkaline ash-fall tuff from Hole #6. Table 1 presents the bulk density, grain density and porosity of these samples. The ash-flow tuff, which extends from 1300 ft to 1346 ft, exhibits a wide range in bulk density and porosity. Table 2 shows the tensile strength, elastic constants and p and s wave velocities of these samples. The tensile strength and elastic constants are determined from direct pull tests, and the p and s wave velocities are determined under zero loading conditions. Note that the densely-welded tuff has a modulus of elasticity an order of magnitude greater than the ash-fall tuff. The criterion distinguishing welded tuffs from other tuffs is often given as (1) density greater than 2.1 gm/cc; (2) compressional strength greater than 5000 psi, and; (3) p wave velocity greater than 9000 ft/sec.

Table 3 presents the permeability as determined from helium gas tests under three loading conditions in as-received and oven-dried states as indicated in the

TABLE 1. Density and Porosity of UEL2gl0#6 Core Samples

Depth (ft)	Type	Bulk Density (gm/cc)		Grain Density (gm/cc)	Porosity %
		Natural	Dry		
1297	Ash-Fall	1.95	1.62	2.49	35.0
1305	Transition	2.12	1.87	2.62	28.7
1313	Transition	1.92	1.57	2.63	40.3
1323	Densely Welded	2.42	2.31	2.65	12.8
1339	Lower Transition	2.18	1.95	2.63	25.7
1343	Lower Transition	2.14	1.97	2.47	20.1
1354	Ash-Fall	1.67	1.23	2.42	49.2
1363	Ash-Fall	1.68	1.24	2.42	48.6

TABLE 2. Tensile Strength, Elastic Moduli and P and S Wave Velocities of UEL2gl0#6 Core Samples

Depth	Type	Tensile Strength psi	Modulus of Elasticity x 10 <sup>6</sup> psi	Poisson's Ratio	Bulk Modulus* x 10 <sup>6</sup> psi	Shear Modulus** x 10 <sup>6</sup> psi	P Wave Velocity ft/sec	S Wave Velocity ft/sec
1297	Ash-Fall	35	1.22	0.213	0.71	0.50	9450	4870
1305	Transition	126	2.12	0.218	1.25	0.87	10100	5510
1313	Transition	108	0.80	--	--	--	7900	4430
1323	Densely Welded	820	5.07	0.213	2.94	2.09	14670	7080
1338	Lower Transition	555	2.35	0.194	1.28	0.98	10800	5880
1343	Lower Transition	29	2.20	0.265	1.56	0.87	11540	6280
1354	Ash-Fall	20	0.81	0.332	0.8	0.30	6190	3450
1363	Ash-Fall	39	0.30	0.206	0.17	0.12	5160	3130

\* Calculated from  $\frac{E}{3(1 - 2\nu)}$

\*\* Calculated from  $\frac{E}{2(1 + \nu)}$

where E = Modulus of Elasticity

ν = Poisson's Ratio

TABLE 3. Permeability of UEL2gl0#6 Core Samples

Depth	Formation	Confining Pressure, psi	Permeability As-Received, md	Permeability Oven-Dried, md
1297.0	Ash-Fall	0	1.3 - 2.4	3.9
		500	0.017	0.21
		1000	0.007	0.11
1305.5	Transition	0	-	2.3
		500	0.19	1.6 - 2.1
		1000	0.33	1.2 - 1.7
1313.0	Cracks and Voids	0	150	235
		500	10	70-85
		1000	18-25	60-75
1323.0	Densely Welded	0	0.006	0.018
		500	0.000	0.005
		1000	0.000	0.002
1339.0	Lower Transition	0	3.7	2.6 - 4.3
		500	0.35	1.3
		1000	0.16	1.0
1343.0	Lower Transition	0	0.004	0.066
		500	0.000	0.027
		1000	0.000	0.009
1354.0	Ash-Fall	0	1.3 - 1.6	4.8 - 6.4
		500	0.17	1.9 - 3.0
		1000	0.20	1.2 - 1.6
1363.0	Ash-Fall	0	0.56	-
		500	0.008	1.2 - 2.4
		1000	0.042	-

\*Sample tested in the order: As-received: 500, 1000, 0 psi; then Oven-dried: 500, 1000, 0 psi

Table. For competent ash fall and welded tuff samples, the permeability is very low. The transition zones typically are fractured and contain many voids and breccia, resulting in high permeability.

The logging service company (Birdwell) ran 3D velocity, density, and caliper logs, and calculated the material properties. Figure 8 shows the p wave and s wave velocities, porosity, and Poisson's ration (solid lines) compared to the core sample results (data points). Figure 9 shows the elastic moduli and bulk density for the 3D log results and core results. With the exception of Poisson's ratio, the correlations are quite good.

#### V. IN SITU STRESSES

The in situ stresses are the parameters that most affect the direction of a hydraulic fracture. It is clear that in a homogeneous medium, the plane of the

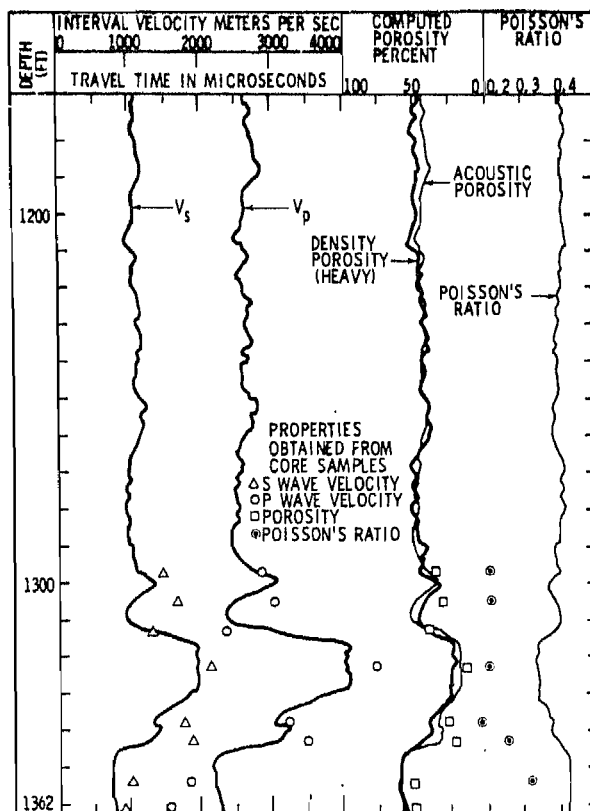


Figure 8. 3D Log Results Compared to Core Sample Results from UE12g10#6.

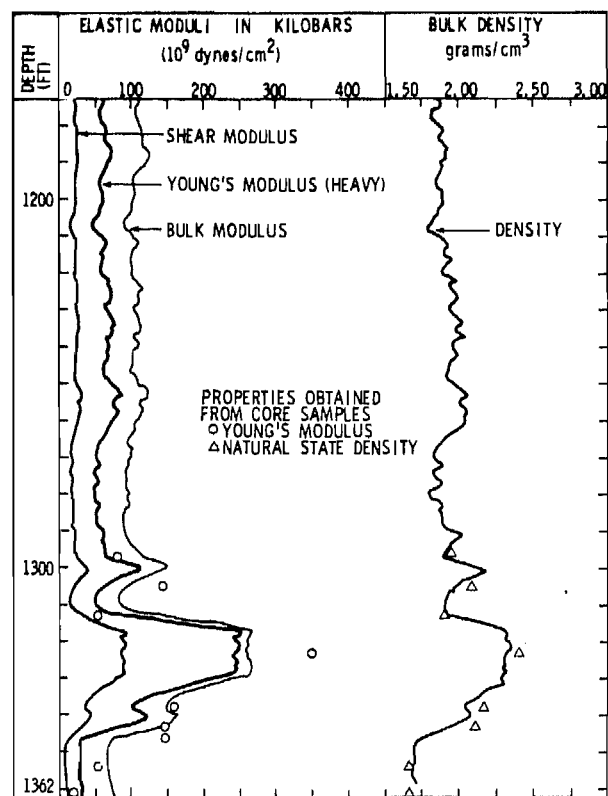


Figure 9. Elastic Moduli and Bulk Density Data from Logs and Cores of UE12g10#6.

fracture will be perpendicular to the direction of the least principal stress. In practice, this should also be true if the non-homogeneities are not overwhelming and the difference between the minimum in situ stress and the other two principal stresses is sufficient. Recently, Simonson, *et al*<sup>12</sup> suggested that differences in the in situ stresses of two materially different, neighboring zones should be a factor in determining whether a fracture will break into the other zone.

In order to fully characterize the fracturing medium, the in situ stress distribution must be determined. Previously, Hooker, *et al*<sup>24</sup> and Miller, *et al*<sup>25</sup> conducted overcore borehole deformation tests in Rainier Mesa to obtain the tectonic stress. Ellis and Ege<sup>22</sup> conducted the same tests in U12g tunnel at the locations designated in Fig. 4 as the "permanent stress station".

Haimson, *et al*<sup>26</sup> and Miller<sup>27</sup> subsequently obtained in situ stresses in Rainier Mesa by hydraulic fracturing. Hubbert and Willis,<sup>28</sup> Kehle,<sup>29</sup> Obert and Duvall,<sup>30</sup> and Haimson and Fairhurst<sup>31</sup> discuss the determination of the stresses via this method. Essentially, if it is assumed that the borehole is parallel to one of the principal stresses and the fluid is non-penetrating, then

$$\sigma_{\max} = 3\sigma_{\min} - P_c + \sigma_T \quad ,$$

where  $\sigma_{max}$  is the maximum principle in situ stress,  $\sigma_{min}$  is the minimum principle in situ stress,  $P_c$  is the breakdown or critical pressure and  $\sigma_T$  is an appropriate tensile strength (values of 309<sup>1</sup> and 435 psi<sup>26</sup> have been measured for the ash-fall tuff).  $\sigma_{min}$  can be determined from

$$\sigma_{min} = P_{isi}$$

where  $P_{isi}$  is the instantaneous shut-in pressure. Employing this method, Tyler and Vollendorf<sup>1</sup> determined the in situ stresses at locations designated HFS #3 through HFS #15 in Fig. 4, as well as UE12g10#3, and they subsequently performed breakdown tests at HFS #17, HFS #18, HFS #19, U12gUG3, and U12gUG3A. Recently, tests were conducted in HFS #20, HFS #23, and EV5 #2, and data are available from the hydraulic fractures in UE12g10#5 and UE12g10#6. These data are shown in Table 4.

TABLE 4. In Situ Stresses Measured in U12g Tunnel

A. Tyler and Vollendorf <sup>1</sup>		
HOLE	$\sigma_{min}$ (PSI)	$\sigma_{max}$ (PSI)
HFS-3	100	
HFS-4	182	545
HFS-5	249	
HFS-6	276	
HFS-7	-	
HFS-8	450	
HFS-9	488	
HFS-10	875	
HFS-11	933	
HFS-12	875	1821
HFS-13	495	
HFS-14	440	
HFS-15	453	1080
UE12g10#3	1114	1898
UE12g10#3	1015	1788
Overcore	377	1233

B. Tyler and Vollendorf (unpublished)

HOLE	Distance from Collar (ft)	$\sigma_{min}$ (PSI)	$\sigma_{max}$ (PSI)
HFS-17	66	938	
	46	950	
	13	1033	
HFS-18	63.5	1700	
	50	1525	
	15	-	
HFS-60	60	725	
	42	-	
	21	-	
U12g10UG3A	286	675	
	236	-	
	217	325	
	135	700	
U12g10UG3	38	425	
	250	787	
	225	300	
	124	1000	
	109	-	
	83	625	
	53	310	

C. Recent Tests

Hole	Distance from Collar (ft)	$\sigma_{min}$ (PSI)	$\sigma_{max}$ (PSI)
HFS #20	66	735	
	46	760	
	26	640	
	8.5	180	
HFS #23	126	683	
	99	454	
	71	700	
	54	714	
	42	571	
	23	400	
	9	686	
EV5 #2	129	476	
	119	468	
	111	498	
	100	570	
	78	684	
	58	643	
	33	570	
	20	655	
12	554		
UE12g10#5	1398	1200	
UE12g10#6	1354	400	770
	1326	430	880

VI. FRACTURE DESIGN

On July 8, 1977, a second meeting with Dowell was held in Albuquerque, NM to finalize the design of the experiment. It was decided that each zone of the tuff be fractured separately with a Nevada "A" cement containing 1% D-60 mixed at 15.4 lbs/gal. This cement was suggested by Dowell because it is a high

water content system that does not become immobilized until 10-12% of the mix water has been lost. It should, therefore, remain fluid and be similar to normal fracturing fluids (except for its high density), allowing the normal fracture propagation process to develop. Dowell also suggested that the resultant set fracture should maintain 90% of the width attained during propagation. The properties are shown in Table 5.

In order to give the fracture sufficient time and length to interact with the interface, it was proposed that Dowell should attempt to propagate a 50 foot high vertical fracture, with 300 foot wings, in both zones. Given the "reservoir" properties in Table 6, Dowell provided fracture design plans for both zones. In the ash-fall tuff, the formation would be broken down with 30 barrels of water. The fracture would be extended by 8000 gallons of grout pumped into the formation at 6 bbls/min in two stages: 4000 gal of green cement followed by 4000 gal of black cement. The different colors would hopefully provide some information on fluid movement and fracture propagation during the operation. The grout would be followed immediately by a displacement of 10 barrels of water. This design should provide a fracture width of about 0.4 in. at the wellbore.

The welded tuff, which is considerably harder and stronger than the ash-fall tuff, would first be notched to insure that the fracture initiates in the welded zone. The formation would again be broken down with water, but only 5000 gallons of blue cement would be injected (also at 6 bbls/min). The grout would again be displaced with 10 barrels of water. This fracture should only have a width of about 0.15 in at the wellbore, principally due to the higher modulus of the welded tuff.

The fracture designs, as given above, are for a homogeneous media with the properties given in Table 6. The interface between the welded and ash-fall tuffs, however, is not well defined. The rock properties vary widely over a ten foot transition interval in which there are many voids, fractures and breccia. Since it is necessary to propagate through this transition zone in order to break into the opposing formation, the behavior of the fracture as a function of reservoir properties has been investigated. The fracture models of Perkins and Kern<sup>33</sup> (modified to include fluid leakoff) and Geertsma and de Klerk<sup>34</sup> have been employed in a parametric study of bulk and matrix rock properties on fracture propagation.

For the purpose of comparison, Fig. 10 shows how the fracture length will increase with injected volume for three different theories. Table 7 shows the data used for these base case calculations. This data is taken from the rock

TABLE 5. Properties of Nevada "A" Cement with 1% D-60 Mixed at 15.4 lbs/gal

Yield	1.21 ft <sup>3</sup> /sack	
Viscosity (apparent)	128 centipose	
$\eta'$	0.86	Pseudoplastic Behavior
$K'$ (not corrected)	0.0031 lb-sec <sup>n'</sup> /ft <sup>2</sup>	
$\eta$	0.07 lb <sub>m</sub> /ft-sec	
$\tau_Y$	0.23 lb/ft <sup>2</sup>	Bingham Plastic Behavior
$C_w$	4.1 x 10 <sup>-3</sup> ft/ $\sqrt{\text{min}}$	
Spurt Loss	0	

TABLE 6. Material Properties for Design Calculations

	Ash Fall Tuff	Welded Tuff
Bulk Density (GM/CC)	1.77	2.37
Grain Density (GM/CC)	2.42	2.6
Porosity (%)	44.6	13
Water Saturation %	100	100
Modulus of Elasticity (PSI)	2.36 x 10 <sup>5</sup>	3.8 x 10 <sup>6</sup>
Bulk Modulus (PSI)	2.21 x 10 <sup>5</sup>	2.44 x 10 <sup>6</sup>
Shear Modulus (PSI)	1.11 x 10 <sup>5</sup>	1.5 x 10 <sup>6</sup>
Poisson's Ratio	0.312	0.238
Permeability (Millidarcies)	0.01	0.02 - 2.0

TABLE 7. Data for Base Case Fracture Calculations

Height	50 ft	
Flow Rate	6 bbls/min	
Viscosity	128 centipose	
Poisson's Ratio	0.312	
Young's Modulus	2.36 x 10 <sup>5</sup> psi	
Spurt Loss	0	
Permeability	0.01 md	
Porosity	44.6%	} Replaced by $C_{vw} = 0.000115$ ft/ $\sqrt{\text{min}}$
Leakoff Viscosity	1 centipose	
Reservoir Viscosity	1 centipose	
Reservoir Compressibility	3.3 x 10 <sup>-6</sup> in <sup>2</sup> /lb	
Treating Pressure Gradient	2400 psi	

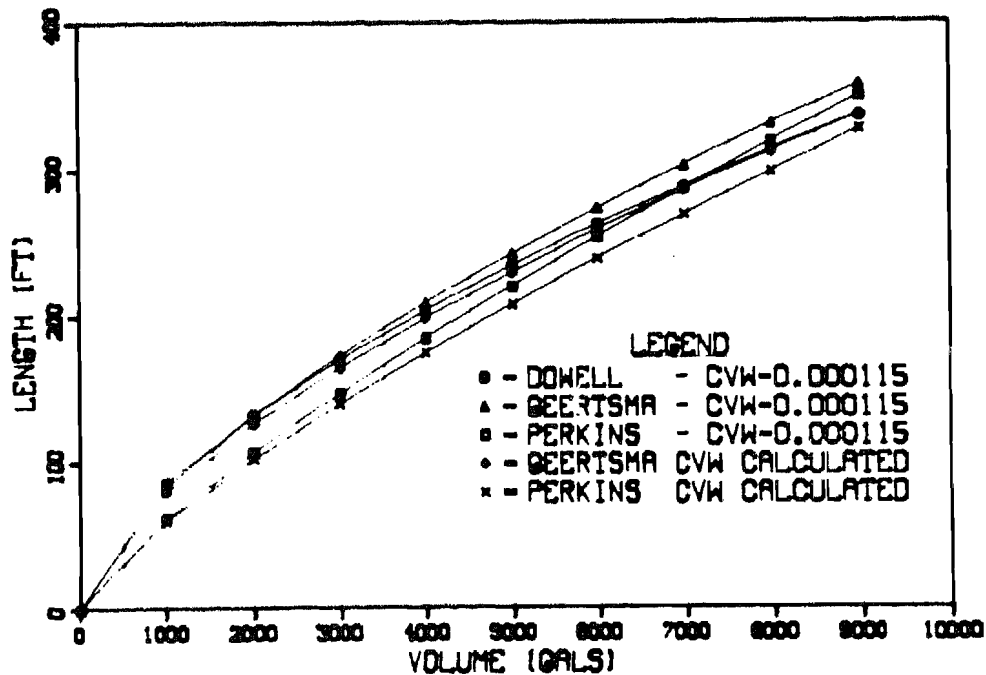


Figure 10. Fracture Length VS Injected Volume.

properties of the ash fall tuff. The loss coefficient ( $C_{vw}$ ) used by Dowell (0.000115 ft/min) has been replaced in a number of calculations by a loss coefficient determined from the last six items of reservoir data given in Table 7. Figure 10 indicates that 8000 gallons of grout will be sufficient to propagate the fracture 300 feet in the ash-fall tuff regardless of the theory used or how  $C_{vw}$  is calculated. More importantly, the effect of fracture propagating in a transition region of widely differing material and reservoir properties must be addressed.

Since the actual fracture operation in the ash-fall tuff utilized 9000 gallons of grout, Figs. 11, 12, 13, 14, and 15 show the effects of various material properties on fracture length for an injected volume of 9000 gallons. Young's modulus, as determined from core samples, is greater in the transition region than in the ash-fall tuff, and Fig. 11 indicates that, if anything, the fracture would tend to propagate farther in the transition region. Figures 12 and 13 show that Poisson's ratio and porosity have little effect on fracture length. The most pronounced effect will arise with permeability differences, as seen in Fig. 14. In tight reservoirs that are 100% saturated, the fluid leakoff should be very small, and consequently the fractures will be considerably longer. However, as the permeability becomes greater, leakoff increases accordingly, and the fracture will be much shorter. For very large permeabilities, the wall building nature of the

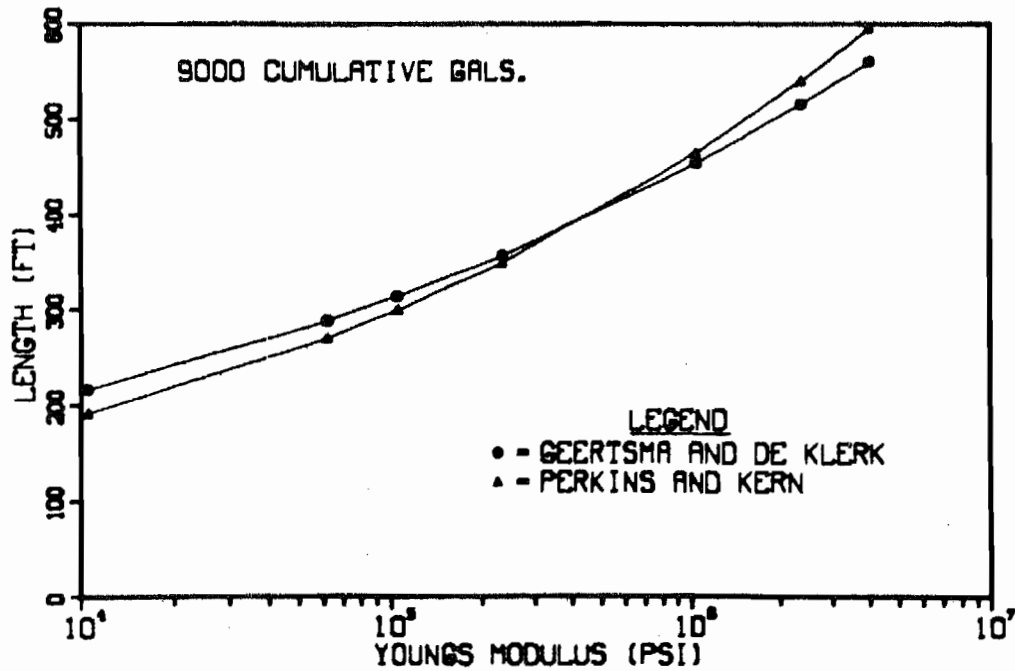


Figure 11. Fracture Length VS Young's Modulus.

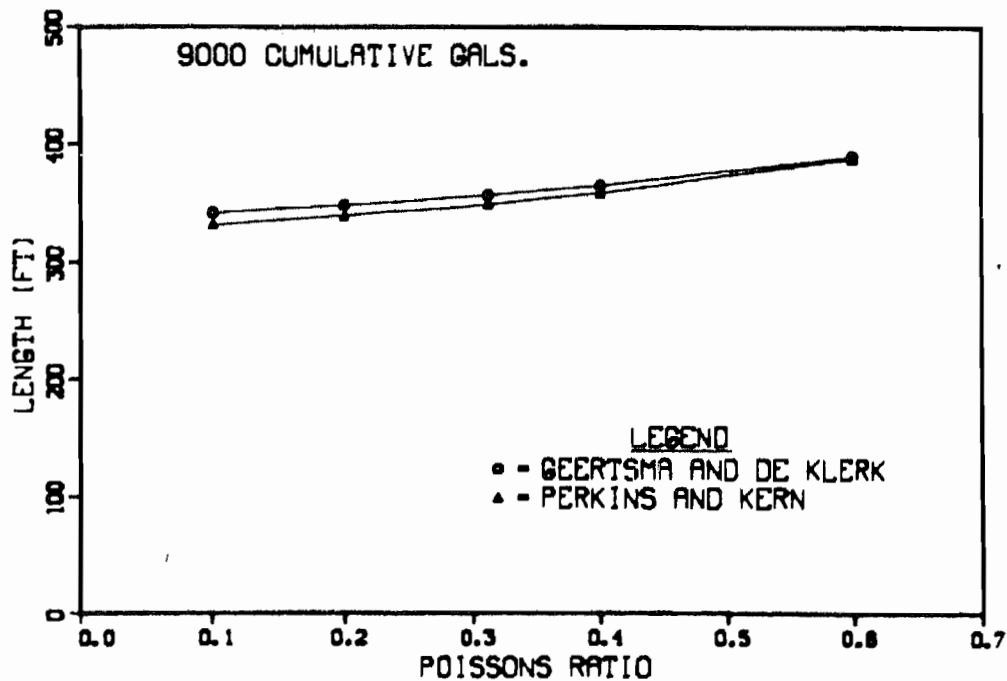


Figure 12. Fracture Length VS Poisson's Ratio.

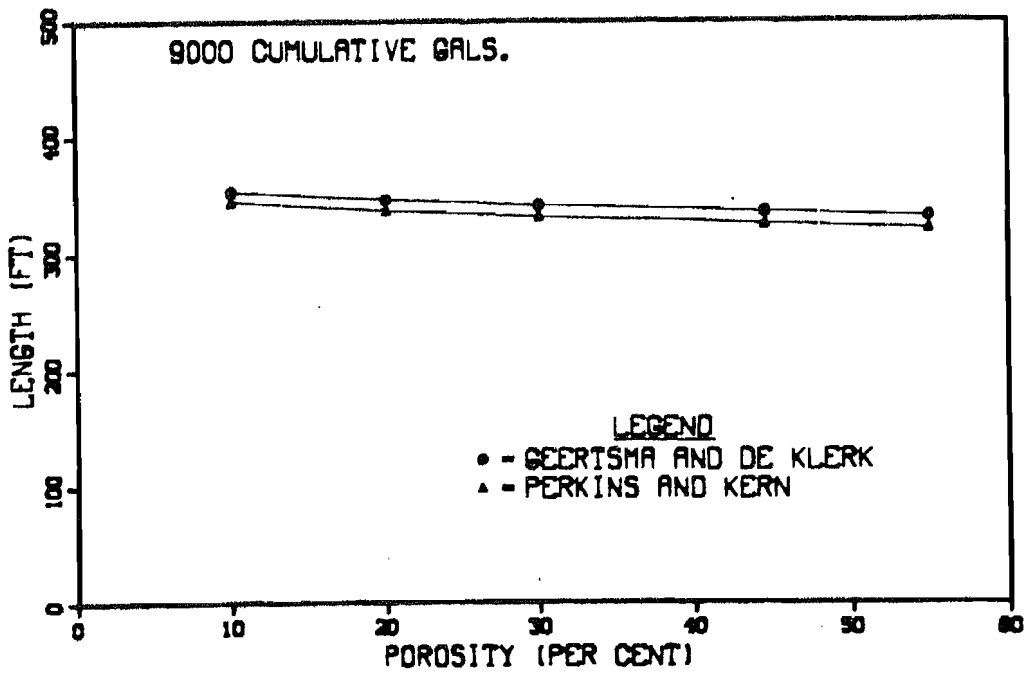


Figure 13. Effect of Porosity on Fracture Length.

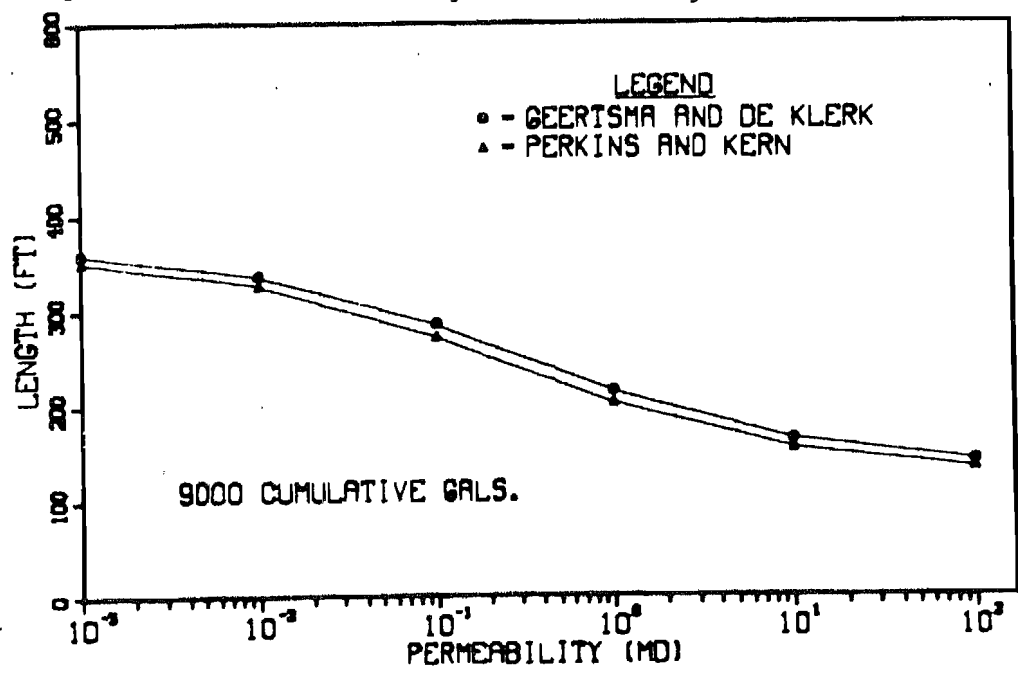


Figure 14. Effect of Permeability on Fracture Length.

fracture fluid becomes dominant, and there tends to be a minimum length for a fracture. This minimum length can be obtained by extrapolating the curve in Fig. 15 out to the value of the wall building coefficient (0.0041 ft/ min). In a real reservoir, however, there may be large scale fractures that will not be clogged by the frac fluid, so that the fluid leakoff may be greater and the fracture may be shorter. This is an obvious problem in attempting to propagate the fracture through the transition region.

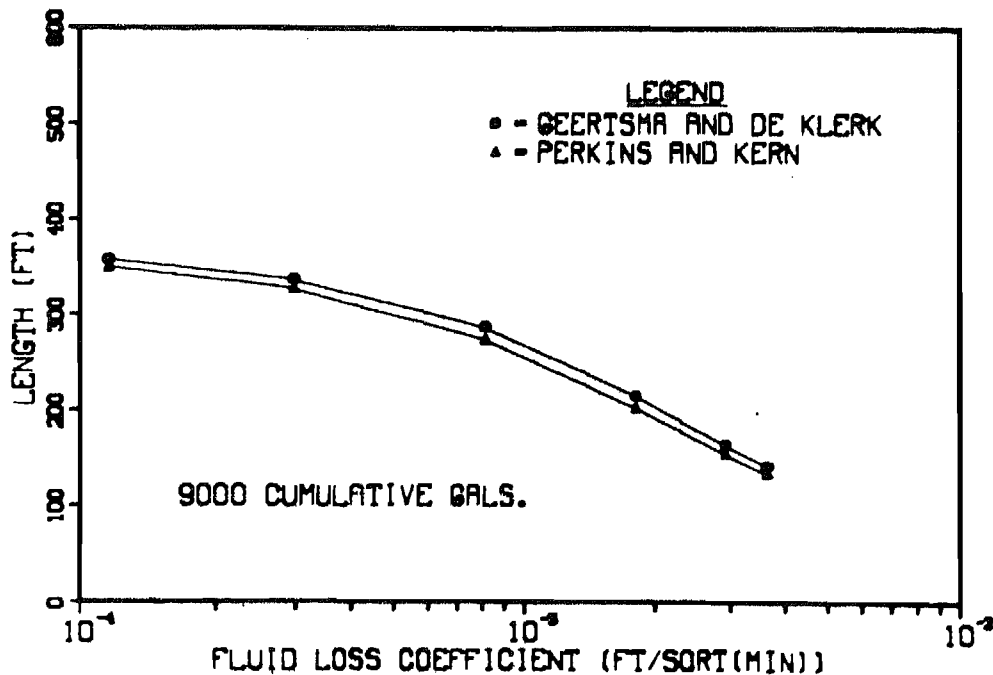


Figure 15. Effect of Loss Coefficient on Fracture Length.

The fracture design for the welded tuff zones was complicated somewhat because the value of the bulk permeability is not well established. The matrix permeability is on the order of 0.02 millidarcies (md) but the overall permeability may be as high as 2 md. Figure 16 shows fracture length versus injected volume for  $C_{vw} = 0.000080$ , which corresponds to a permeability of 0.02 md. (The data for these calculations is shown in Table 8). It is obvious that if the permeability is less than 0.2 md, 5000 gallons of grout will be sufficient, as shown in Fig. 17. For the case where the permeability is 2.0 md, Dowell gives a fluid loss coefficient of 0.000796 ft/min, and for this leakoff, 5000 gallons of grout is sufficient. Using the reservoir data given in Table 8 to calculate the leakoff, it can be seen in Fig. 18 that the wings may be considerably shorter than expected.

It is also interesting to compare the differential fracturing pressure (fracturing pressure - minimum in situ stress) predicted by both theories for the two zones. As shown in Fig. 19, the differential pressure necessary to fracture the welded tuff is an order of magnitude greater than that necessary to fracture the ash-fall tuff. As is often noted in the literature, Perkins and Kern<sup>33</sup> expect the pressure to rise during fracturing and Geertsma and de Klerk<sup>34</sup> expect the opposite.

It should also be mentioned that grout is considerably different from a normal fracturing fluid. The rheological curves for the three different-colored cements are shown in Figs. 20, 21, and 22. Shear stresses for strain rates of 100,

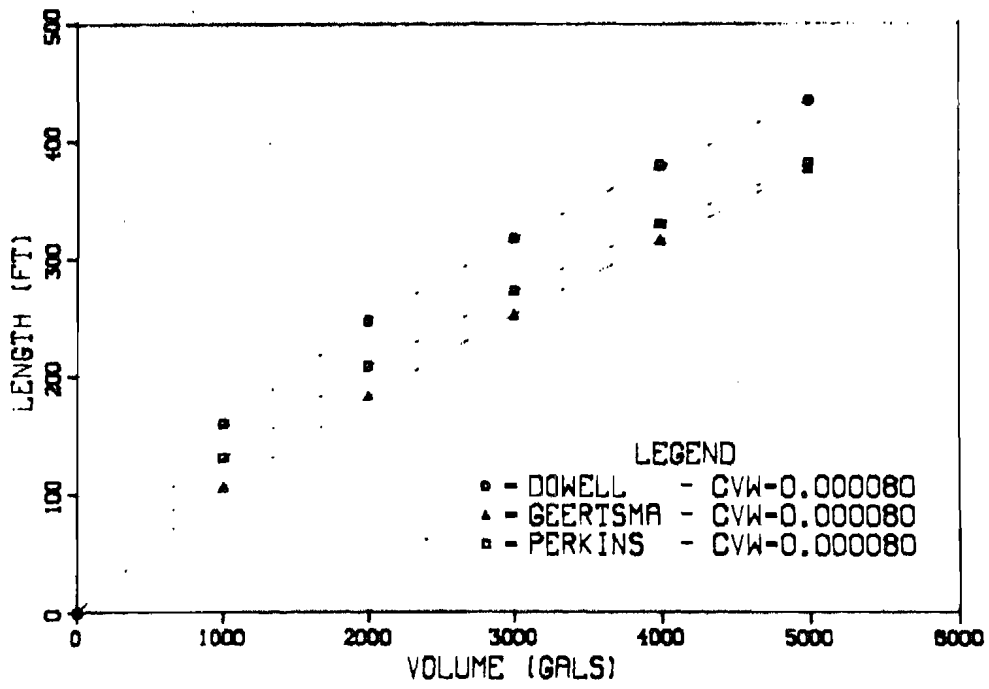


Figure 16. Fracture Length VS Injected Volume.

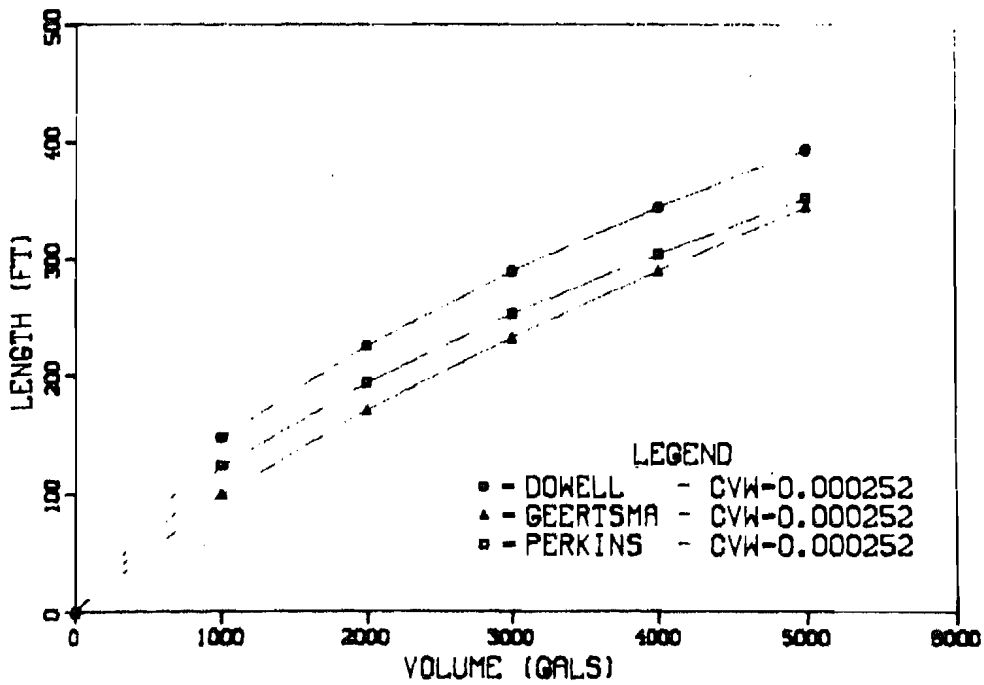


Figure 17. Fracture Length VS Injected Volume

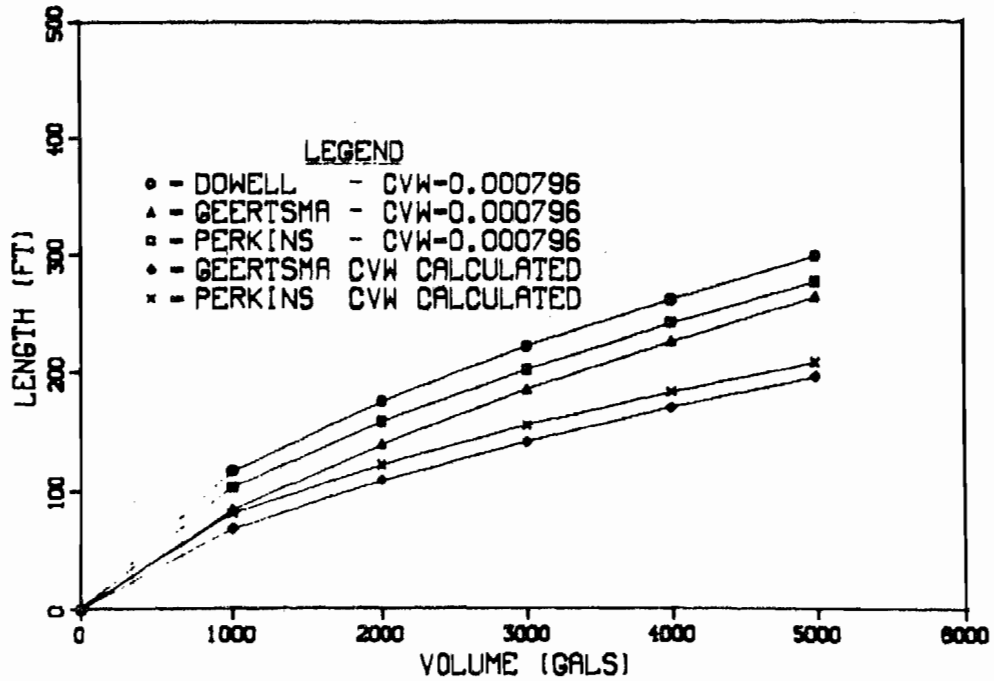


Figure 18. Fracture Length VS Injected Volume.

TABLE 8. Data for Welded Tuff Fracture Calculations

Height	50 ft	
Flow Rate	6 bbls/min	
Viscosity	128 centipoise	
Poisson's Ratio	0.238	
Young's Modulus	$3.8 \times 10^6$ psi	
Spurt Loss	0	
Permeability	2.0 md	} Replaced By
Porosity	13%	
Leakoff Viscosity	1 centipoise	
Reservoir Viscosity	1 centipoise	
Reservoir Compressibility	$3.3 \times 10^{-6}$ in <sup>2</sup> /lb	
Treating Pressure Gradient	2400 psi	$C_{vw} = 0.000796$ ft/ $\sqrt{\text{min}}$

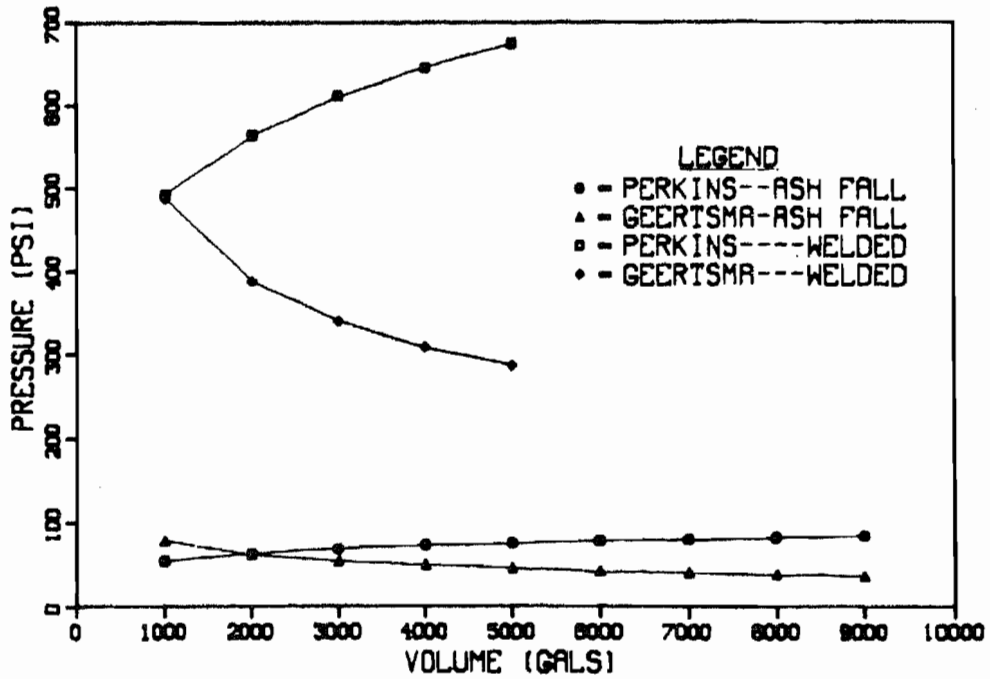


Figure 19. Differential Pressure VS Injected Volume

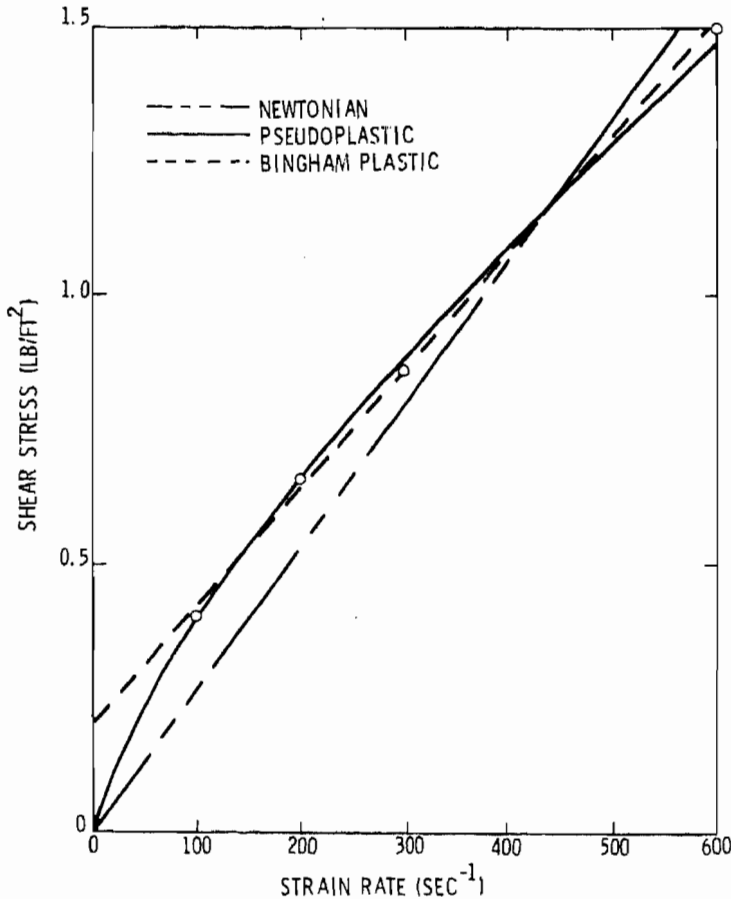


Figure 20. Rheological Properties of Green Nevada "A" Cement + 1% D60 Mixed at 15.4 lb/gal. (O Measured Values)

200, 300 and 600  $\text{sec}^{-1}$  were obtained by Dowell, and the best fit curves for Newtonian, pseudoplastic, and Bingham plastic behavior are indicated as well as the best fit for all the data as shown in Fig. 23. The apparent viscosities ( $\mu_{app}$ ), absolute consistencies ( $K$ ), flow behavior indexes ( $n$ ), yield stresses ( $T_y$ ) and coefficients of rigidity ( $\eta$ ) are given in Table 9.

Perkins and Kern<sup>33</sup> derive width equations for a Newtonian fluid and a pseudoplastic with no leakoff. A width equation for a Bingham plastic can also be derived, and all three equations can be modified to account for leakoffs. For small leakoff rates

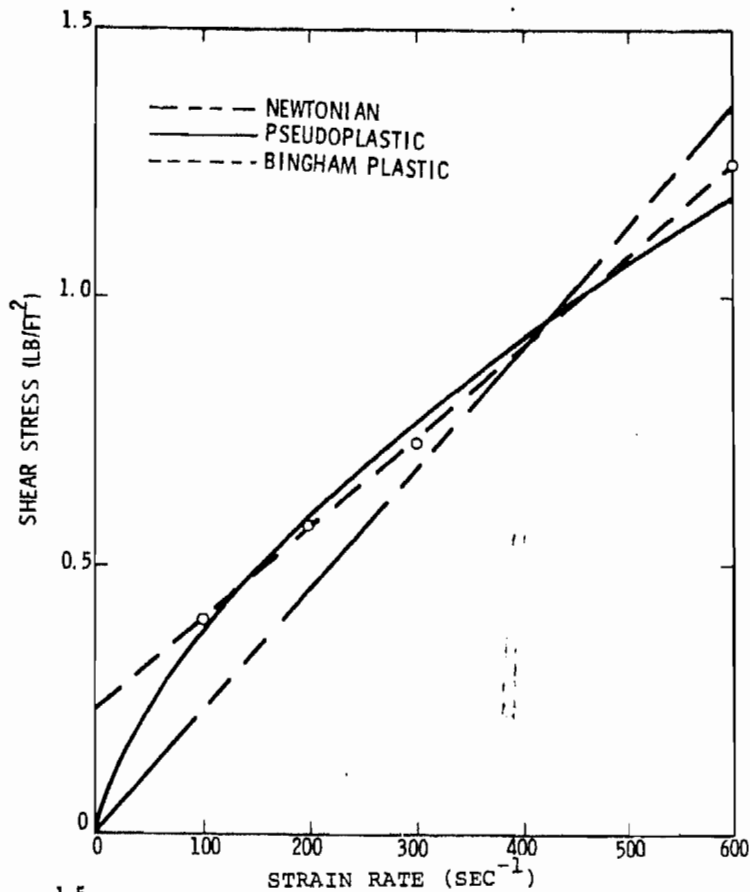


Figure 21. Rheological Properties of Black Nevada "A" Cement + 1% D60 Mixed at 15.4 lb/gal (○ Measured Values).

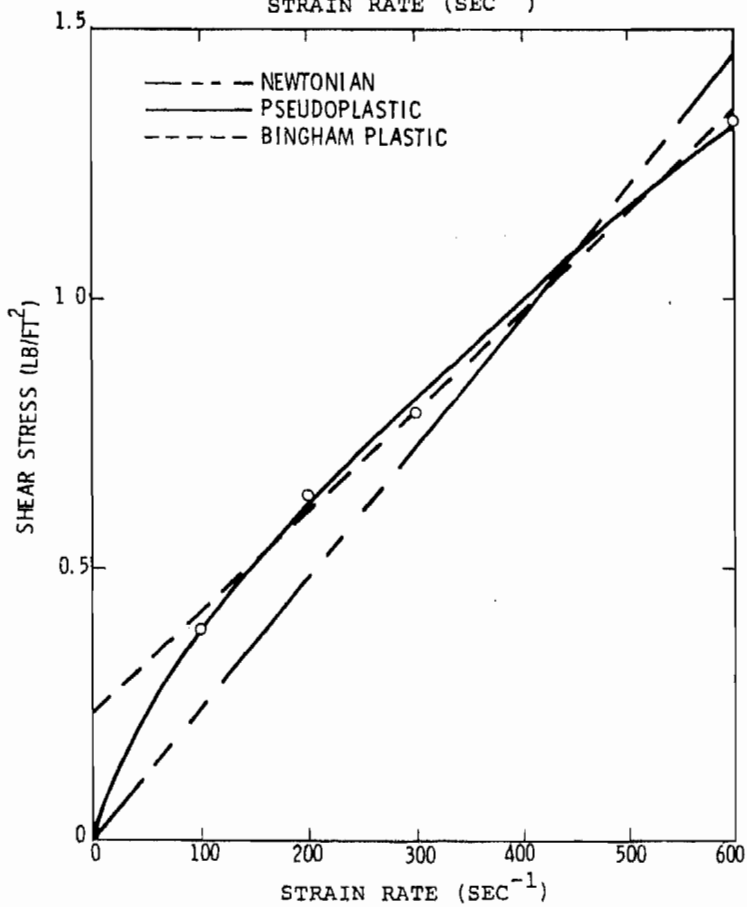


Figure 22. Rheological Properties of Blue Nevada "A" Cement + 1% D60 Mixed at 15.4 lb/gal (○ Measured Values).

TABLE 9. Derived Fluid Constants for the Fracturing Fluid

Color	Newtonian	Pseudoplastic		Bingham Plastic	
	$\mu_{app}$ (cp)	$\eta'$	$K' (\text{Lb-sec}^{n'} / \text{ft}^2)$	$\tau_y (\text{lb/ft}^2)$	$\eta (\text{lb}_m / \text{ft-sec})$
Green	127.5	0.73	0.0138	0.206	0.0697
Black	107.7	0.63	0.0213	0.232	0.0544
Blue	115.3	0.68	0.017	0.235	0.0594
All	116.8	0.68	0.0171	0.224	0.0612

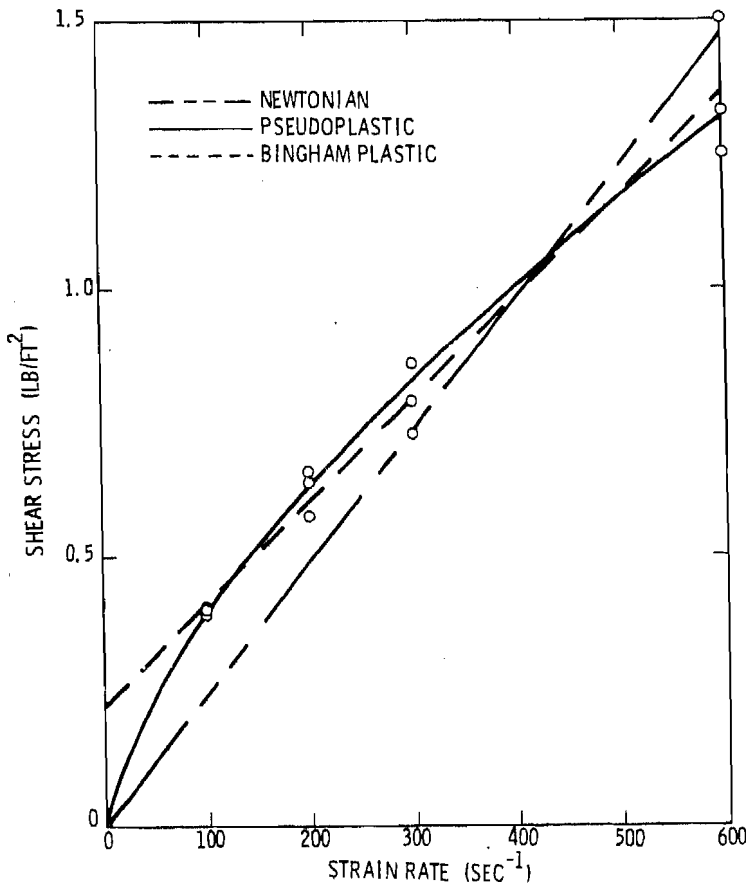


Figure 23. Average Rheological Properties of Nevada "A" Cement + 1% D60 Mixed at 15.4 lb/gal. (O Measured Values)

(as in the case in ash-fall tuffs), this method should be acceptable. Figure 24 shows the rheological effects on fracture length for the ash fall tuff using the base case data of Table 7 with the data from Table 9. The ash-fall tuff has very low moduli which result in large widths and, therefore, low strain rates (20-100  $\text{sec}^{-1}$ ).

As shown in Figs. 20 through 22, the Bingham plastic model provides the best estimate of viscosity for this situation and a more realistic crack length. The pseudoplastic model is suitable for this application: however, with a larger volume (larger widths and lower strain

rates), it would tend to further overshoot the Bingham plastic results. For the welded tuff, the situation is different. The elastic moduli are much larger, the widths are smaller, and therefore the strain rates are larger (300-500  $\text{sec}^{-1}$ ). As shown in Fig. 25, the Newtonian and pseudoplastic models provide a larger apparent viscosity than the Bingham plastic, and therefore, the Bingham plastic model provides the longest fracture.

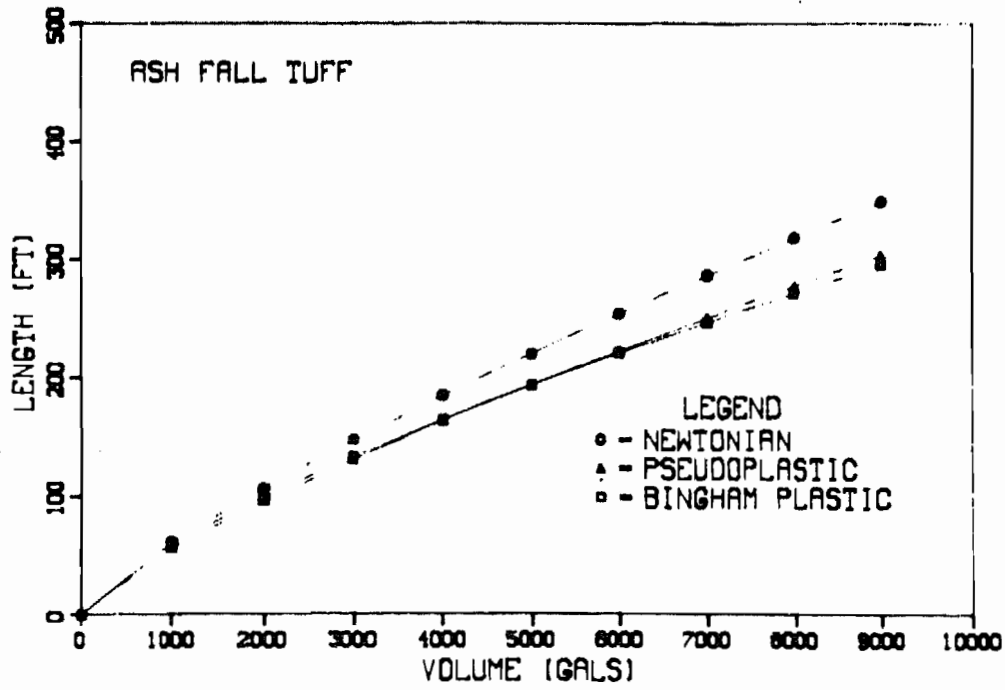


Figure 24. Effect of Rheology on Fracture Length.

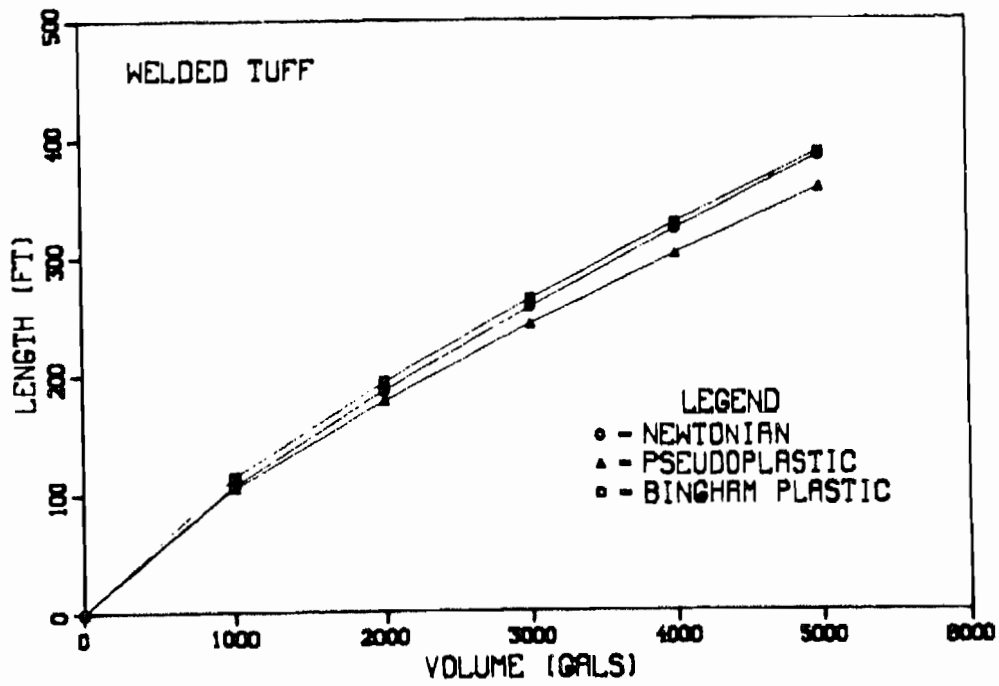


Figure 25. Effect of Rheology on Fracture Length.

## VII. EXPERIMENTAL OPERATIONS

A site for the interface experiment was chosen in May, 1977, and designated UE12g10#6, with surface coordinates of N882,870.34 and E632,160.37, referenced to the NTS coordinate system. A road to the surface location was completed in May, 1977, and drilling operation began in June. The 4 in. diameter well was drilled to a total depth of 1455 ft, with a collar elevation of 7554.76 feet. The entire hole was cored and a large number of samples were waxed; at the end of June, nuclear, density and caliper logs were run. The hole would not hold water, and a velocity log was not obtained.

During July, four instrumentation holes were drilled from the VDH#5 evaluation drift into the ash fall tuff underlying the interface. As shown in Fig. 26 two holes were drilled at S 43°, 44' 18"W and two at S 26° 45' 08"W, with one hole of each set drilled at -5° to 165 feet total depth (TD) and the other drilled at -21° 31' 22" to 175 feet total depth. The direction of these holes is such that at total depth these holes are the vertices of a square 50 feet on edge in a vertical plane, the center of which is approximately 85 feet below the interface. A triaxial geophone package was grouted in each hole at total depth for acoustic signal detection, approximately 200 feet away from UE12g10#6.

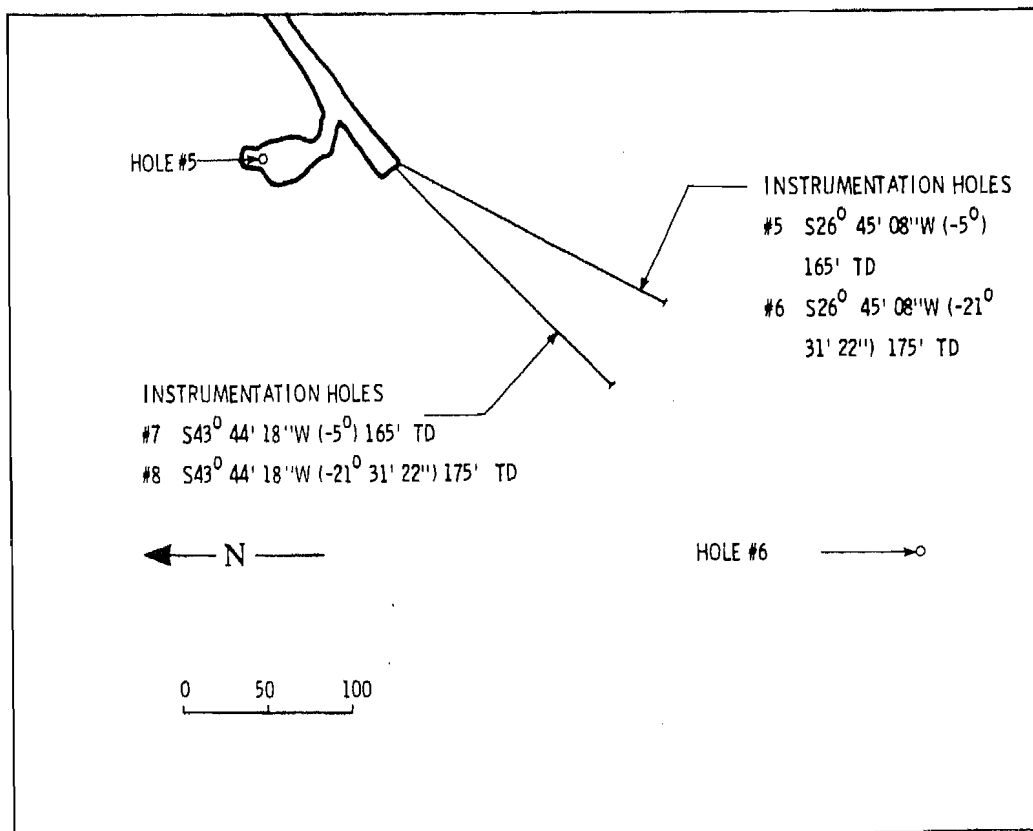


FIG. 26 GEOPHONE INSTRUMENTATION HOLES

### Zone #1 - Ash Fall Tuff

In preparation for the hydraulic fracture, a drilling rig was moved back on to the site on August 17, 1977. The hole was cleaned out to 1450 feet and filled with water. A neutron log was run again, but the hole still would not hold water, and the velocity log was not obtained. NQ rods (2-3/4" O.D., 2-3/8" I.D.) were run in the hole, and pea gravel was spotted to 1365 feet.

The final adjustments of the special downhole pressure transducer were completed on August 22. This transducer was fitted into a specially designed offset I.D. sub that attaches to the top of the packer collar, and it was designed to be hard wired to the surface by taping the wire to the drill string at approximately 10-foot intervals. Provisions were also made for recording the flow rate directly from Dowell's instrumentation and obtaining wellhead pressures from a transducer near the collar. Arrangements had previously been made to lower an Amerada bomb downhole as a backup pressure recording system.

On the morning of August 23, a Lynes production-injection packer was run in the hole on NQ rods and was set at 1500 psi. (This packer utilizes an inflatable packer element and is designed for either permanent or temporary use in open holes or casing. The seal length of the inflatable element is 53 inches and the O.D. is 3-1/2 inches.) The operational plan called for most of the water to be blown out of the tubing, but the available compressor was rated too low to blow out more than 270 feet of water.

At this point, the transducer malfunctioned and it was decided to delay the experiment until this could be remedied. Later in the afternoon, it appeared that the transducers were functioning properly, and the original plans were modified so that the fracture operation could be completed that evening.

First, a sinker bar was dropped on a wireline to knock the shear pin out of the plug retainer sub on the packer. The Amerada pressure bomb was then set for 1-1/2 hours and lowered through the tubing. The bomb tagged bottom at 1358 feet, seven feet higher than expected. Since this left only four feet between the plug retainer sub and the pea gravel top, the 5-1/2 foot bomb was moved above the packer and the transducer sub so that its bottom was situated at 1337 feet. A schematic of the fracture zone is shown in Fig. 27.

The NQ string was filled with water and at 0735, 30 barrels of water, pumped at 5 bbls/min, broke down the formation. No breakdown pressure spike was observed at the drill site, and injection pressures were very low. At this point

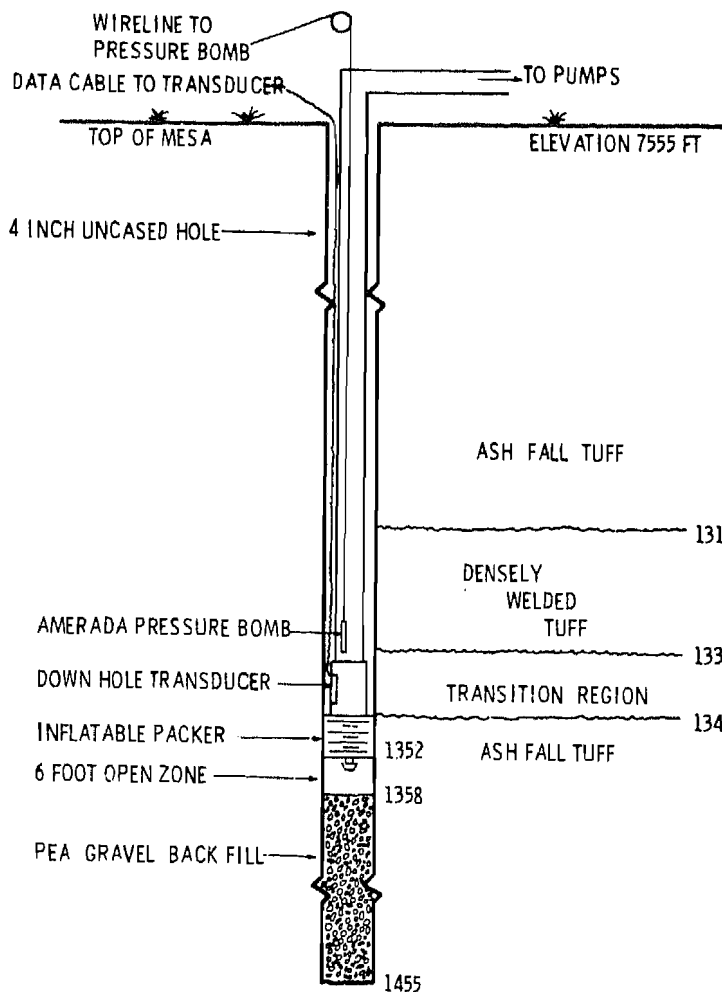


Figure 27. Ash-Fall Tuff Hydraulic Fracture Zone

it was not apparent whether the bottom hole pressure transducer was operating properly; the well-head pressure gage and transducer never functioned properly.

At approximately 0742, Dowell switched to the green slurry. Shortly after this (about 0745), it was observed that the pipes were vibrating acutely and this continued for about 3 or 4 minutes. At about 0800, injection was interrupted for a few minutes so that the acoustic measurement group could change the magnetic tape of their recorder. Dowell injected a total of 128 bbls of green slurry instead of the scheduled 96 bbls.

At 0809, Dowell switched to the black slurry. By this time it was certain that neither the downhole transducer nor the well-head pressure transducer was functioning. At about 0816, Dowell shutdown for about 4 minutes to mix more cement. After re-

starting, the vibrations in the line were again noticed. A total of 90 bbls of black slurry was injected, and at 0830 a flush of 10 bbls of water was initiated. The well was shut in at 0832 for 6 min (until the Amerada bomb had completed its 1-1/2 hour time span), and then the pressure bomb was quickly recovered. Upon removal of the bomb, well operations were suspended for half an hour to provide a quiet period for acoustic measurements. The pressure bomb was quickly checked, and we found it had functioned properly. After the acoustic measurements were completed, the packer was hoisted a short distance upward so that it would not become lodged in the set-up cement. Figure 28 shows the

### HOLE 6 - FORMATION INTERFACE TEST, LOWER FRAC

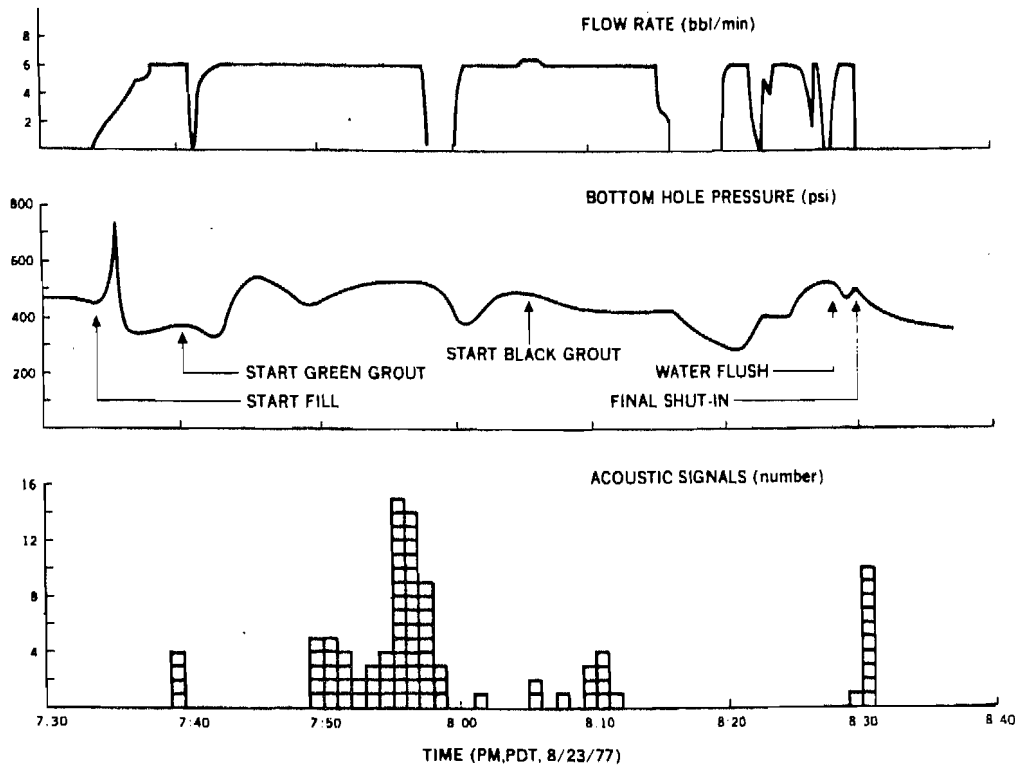


Figure 28. Pressure, Flow Rate, and Acoustic Data for the Ash-Fall Tuff Fracture Interval.

correlated pressure, flow rate and acoustic data from the experiment.

#### Zone #2 - Welded Tuff

The following day, August 24, the drill string and packer were removed from the hole. Dowell then ran an Abrasijet downhole to cut a notch in the dense zone of the welded tuff to insure that the fracture initiated at the proper location. While the tool was being retrieved, a section of pipe (and the Abrasijet) was lost downhole and a fishing operation was initiated to retrieve the string. Various difficulties complicated the fishing operation, but all of the lost pipe and the tools were recovered by the first week in October.

By that time the hole had been reamed from 4 inches to 6-1/4 inches, and T.D. was tagged at 1368 feet. The hole finally held water, so velocity, electric and temperature logs were run, as well as another caliber log; with measurements complete, the hole was backfilled to 1331 ft with pea gravel.

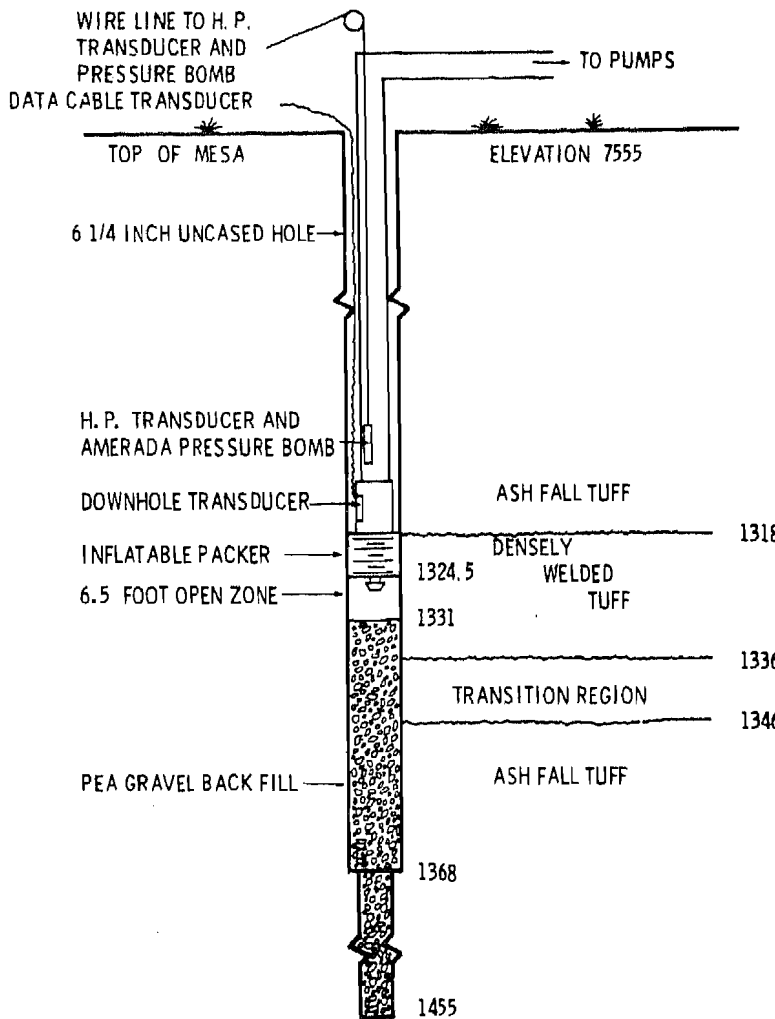


FIG. 29 WELDED TUFF HYDRAULIC FRACTURING ZONE

An Amerada pressure bomb set for three hours and a Hewlett-Packard (HP) quartz crystal oscillator pressure transducer were run downhole on a wireline, with the bottom of the Amerada bomb set at 1300 ft. The HP sensor was 5.2 feet above the Amerada bomb. The hydrostatic pressure was monitored with the HP transducer, and it apparently dropped very slowly from 328 psi to 305 psi, and then leveled off. (Later, it was found that the Amerada bomb showed no pressure decrease at this time, and the dropoff from the HP transducer might have been a temperature drift as the sensor approached thermal equilibrium with the wellbore fluid.) Figure 30 shows the correlated pressure and flow rate data for the breakdown. At 1111, the 2-7/8 in. drill string was filled with water, at as constant a rate as possible, with both the downhole pressure transducers and the geophones recording. When the tubing was full, the hydrostatic pressure remained stable at 562.7 psi,

On October 19, 1977, a Lynes packer was run in the hole on 2-7/8 in tubing. The bottom of the element was positioned at 1324.5 ft, and the packer was set at 1500 psi. The transducer sub was in the drill string above the packer, and the cable was taped at 10 ft intervals to the string. Over half of the water in the drill string was displaced by running a smaller diameter closed-end tubing string inside. After preliminary tests, it was found that the bottom hole pressure transducer in the sub malfunctioned, and it was discarded.

On October 20, 1977, the water level in the drill string was tagged at about 612 ft. The shear pin in the packer was knocked out with a sinker bar, and the bottom was subsequently tagged at 1331 ft. A schematic of the fracture zone is shown in Fig. 29.

indicating that there was no fluid loss to the formation through the packed-off interval. The bottom hole pressure sensors were hoisted to the surface at 1130, and the Amerada bomb was reset for three hours.

The sensors were run down the hole again, and by 1215 preparations were completed for breakdown. Pumping commenced shortly before 1220, and the bottom hole pressure (BHP) rapidly increased to near 1400 psi before a leak in the lubricator at the wellhead forced a shutdown. The BHP dropped to 560 psi and then held constant, indicating that the formation might not have broken down.

Pumping resumed at 1234, and the formation broke down at 960 psi. At 1237, Dowell began pumping at a higher flow rate which induced severe vibrations in the tubing. The signals from the HP transducer were lost at 1238; at 1240.30, the signal was regained for 45 seconds, but then it was lost for the remainder of the breakdown, shut in, and the quiet time that followed. Flow rates were obtained by tapping off Dowell's instrumentation line, and wellhead pressures were obtained from a transducer near the collar. Thirty barrels of water were subsequently pumped into the formation.

The well was shut in for 1/2 hour for acoustic measurements, and at the end of this period, the pressure sensors were brought back to the surface. The HP sensor was examined and it was found that three of the pins on the male connector of the coaxial cable had been jammed into the head. The contact was poorly established, and vibration and strain could easily break the circuit; the pins were pulled back out and the line was reconnected.

The Amerada bomb was reset, and both sensors were run down the hole at 13:20. At 1300 ft, the HP was recording 101 psi and falling as shown in Fig. 31. The pressure dropped to 78 psi by the time a filling-up operation began. The highest level to which the wellbore could be filled was 113 ft (514 psi); at this level the formation took water as quickly as it was poured in. At 1348, Dowell began pumping the blue grout at 6 bbls/min. The signal from the HP sensor was lost again at 1351 and returned only very sporadically until 1356, when it returned for 2 min. At 1358, the lubricator began leaking again, and the pumping was shut down. At this time, the signal was also lost again. After repairing the lubricator, pumping was resumed at 1405. After one minute, the signal from the HP returned and showed a BHP of 700 psi. The pressure increased very slowly until 1416 when it dropped sharply to 560 psi. At 1418, after pumping 117

barrels of cement, Dowell began displacing the grout with 10 bbls of water, and at 1420.30, the well was shut in and a quiet period for acoustic measurements began.

At 1423, the signal from the HP transducer was permanently lost. At about 1435, the quiet period was over, and the pressure sensors were brought to the surface. Later that afternoon the packer was lifted out of the hole, and a temperature survey was run.

#### VIII. RESULTS AND DISCUSSION

The in situ examination of hydraulic fractures near a geologic interface should provide a wealth of observational information. In order to evaluate and draw specific conclusions from the observational data, it is necessary to relate these results to the specifics of the hydraulic fracturing process and the properties of the fracturing medium. One would need to know the geologic structure and material properties of the medium condition of the wellbore (fractured etc.), and properties of the fracturing fluid, as well as obtaining detailed pressure and flow rate data.

Prior to mineback, the available information consisted of core samples, logs, pressure data, flow rate data and acoustic signals. The geologic and material property information has previously been discussed, but it is possible to draw a number of conclusions from the remaining data. Referring to the pressure and flow rate data of Figs. 28, 30, and 31, it should first be noted that in both of the packed-off intervals, the formation was apparently not fractured, since it held the initial water level when the tubing was filled, as is evident from the flat pressure plateaus observed before breakdown in Figs. 28 and 30. The breakdown pressure ( $P_c$ ) in the ash-fall tuff was 730 psi; in the welded tuff the breakdown pressure is somewhat unclear. The wellbore was pressurized to 1400 psi before a leak at the wellhead forced a shutdown. Upon repressurization, the formation completely broke down at 960 psi. It appears likely that the actual breakdown pressure is greater than 1400 psi; however, for later calculations, a  $P_c = 1400$  is employed.

The fracture extension pressure ( $P_f$ ) is a result of a complex interplay among the many fracture parameters. Hopefully, the behavior of  $P_f$  would supply considerable information about the fracturing process, but at the present time, the effects of the various frac parameters are difficult to unravel. Figures 28, 30, and 31 offer some interesting comparisons of these effects.

It is obvious that for a constant flow rate, the fracturing process is similar to the feedback signal of the system. Changes in  $P_f$  reveal the relative

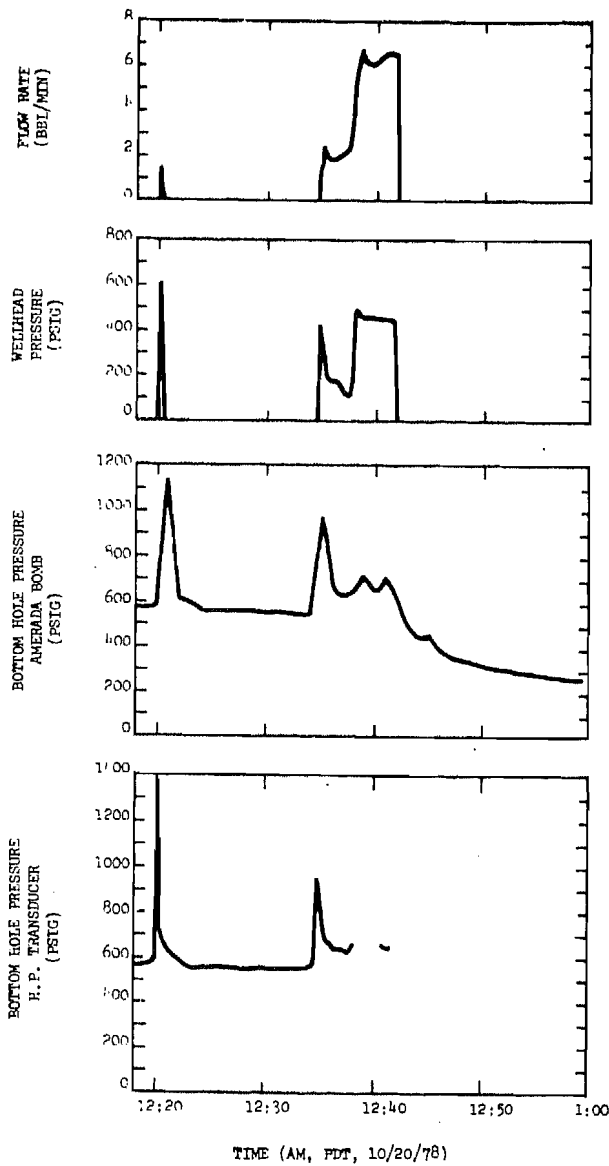


Figure 30. Initial Flow Rate and Pressure Data for the Welded Tuff Fracture Interval.

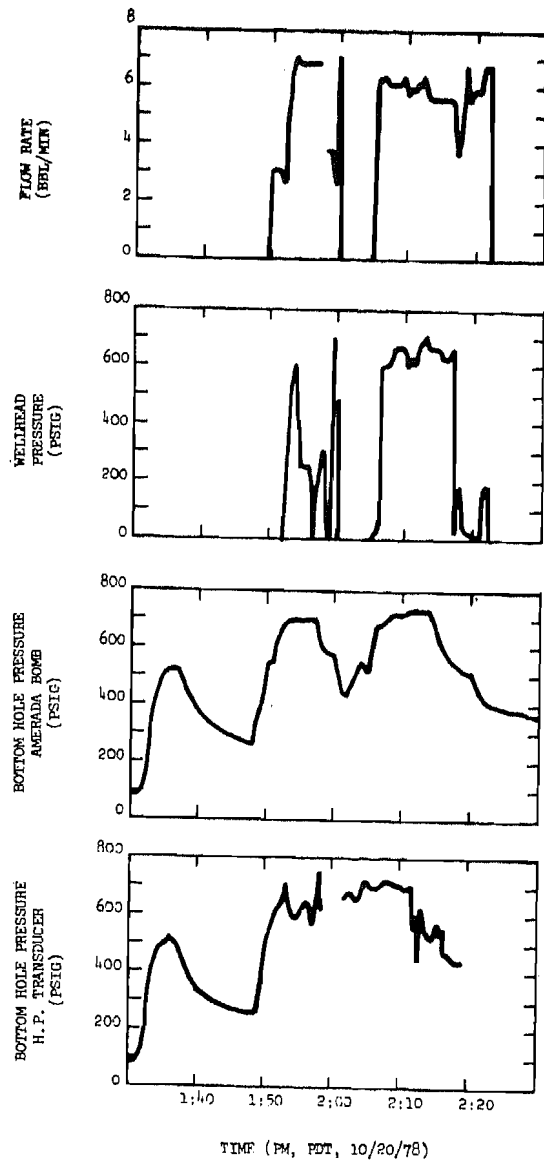


Figure 31. Flow Rate and Pressure Data for the Fracturing of the Welded Tuff Interval.

ease or difficulty of further extension of the fracture due to local variations in material properties, in in situ stresses, in stratigraphy, or many other reasons. For a homogeneous medium,  $P_f$  is the result of the interplay between properties of the medium and properties of the fluid. From a fracture mechanics viewpoint, the extension pressure will decrease with increasing fracture length, but from a fluid mechanics viewpoint, the extension pressure will increase with increasing fracture length. In the ash-fall tuff, where the elastic moduli are an order of magnitude less than the welded tuff moduli, the fracture should have a considerably larger width and therefore much smaller viscous pressure losses. Using the widths

estimated by theory, the average wall shear stress for the ash-fall tuff is only 40% of the value for the welded tuff fracture. This may explain the apparent pressure decrease during fracture extension in the ash-fall tuff compared to the apparent rise in fracturing pressure for the welded tuff. Although it is expected that the pressure would provide clues to the fracturing process, the data of Fig. 28 is difficult to interpret due to the numerous shutdowns. Figure 31 is interesting because of the 100 psi drop in  $P_f$  at 1357 and 200 psi drop at 1414. The same type of pressure decrease would be expected if the fracture broke out of the welded tuff into the ash-fall tuff.

The instantaneous shut in pressure of the fracture in the ash fall zone ( $P_{isi}$ ) is very difficult to determine. The grout in the wellbore is displaced with water before shut in, but the column of water produces a pressure is still 130 psi greater than the lowest fracturing pressure. Thus, it is expected that the fracture would continue to extend for a short time after shut in. Nevertheless, it appears that  $P_{isi}$  is about 400 psi. For the welded zone,  $P_{isi}$  is about 430 psi. Assuming that the minimum principle in situ stress ( $\sigma_{min}$ ) is equal to  $P_{isi}$ , the maximum principle in situ stress ( $\sigma_{max}$ ) can be estimated from

$$\sigma_{max} = 3\sigma_{min} - P_c + \sigma_T$$

where  $\sigma_T$  is an appropriate tensile strength of the material, the fracturing fluid is non-penetrating and the pore pressure is zero. For the ash-fall tuff  $\sigma_T = 300$  psi is commonly employed so that  $\sigma_{max} = 770$ . For the Grouse Canyon welded tuff, there is no accepted value of  $\sigma_T$ . If it is assumed that the tensile strength of the welded tuff relative to the ash-fall tuff is approximately the same as the compressive strength ratio, then  $\sigma_T$  for the welded tuff is 3.3  $\sigma_T$  of the ash-fall tuff or 990 psi. Thus, a  $\sigma_{max}$  of 880 psi is calculated. The orientation of the principle stresses should be evident during mineback. Should it be observed that the fractures change direction, then further in situ stress tests via overcoring or small breakdown experiments will be conducted to determine if this is a result of in situ stress (magnitude or orientation) variations. Special attention will be given during mineback to the angle at which a fracture approaches the interface or bedding planes and the subsequent effect on the fracture. Attention will also be given to the degree of bonding of these planes.

In hydraulic fracturing operations, the fracture is usually expected to propagate upward since the density of the fluid is less than the gradient of the minimum principal in situ horizontal stress. In the ash-fall zone, however, the tuff

density varies from 1.4 to 2.0 gm/cc and the fluid density of 1.9 gm/cc is, in general, greater than the lithostatic gradient. This suggests the lower fracture may propagate downward. In the welded tuff, the grout's density is less than that of the formation.

As shown in Fig. 32, temperature surveys were run in the open hole before the second zone was fractured and again about four hours later after the tubing was pulled out. The effect of the grouted fractures, 1324 ft to the top of the pea gravel back fill, is evident in the post-test survey.

Preliminary results<sup>35</sup> of the acoustic data generated by the first fracture have been obtained by examining the source locations determined from the P-wave and S-wave difference arrival times received

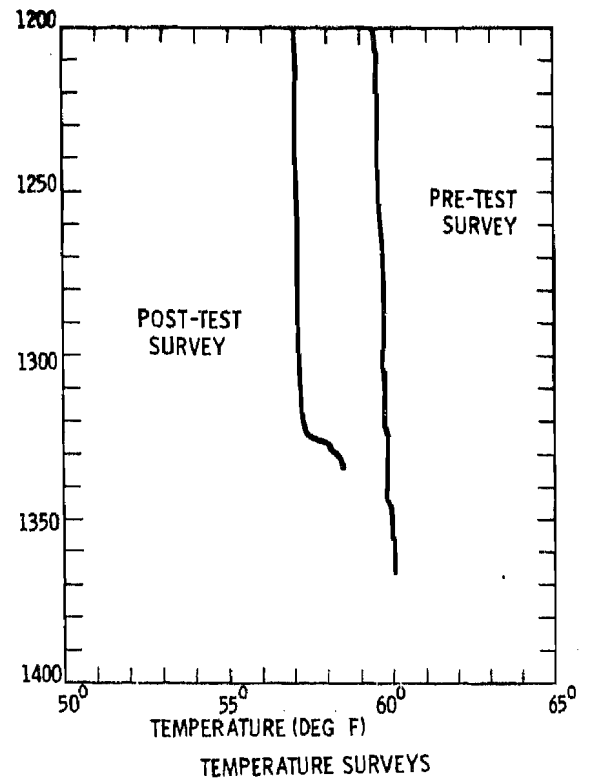


Figure 32. Temperature Surveys Before and After Fracturing to the Welded Tuff Interval.

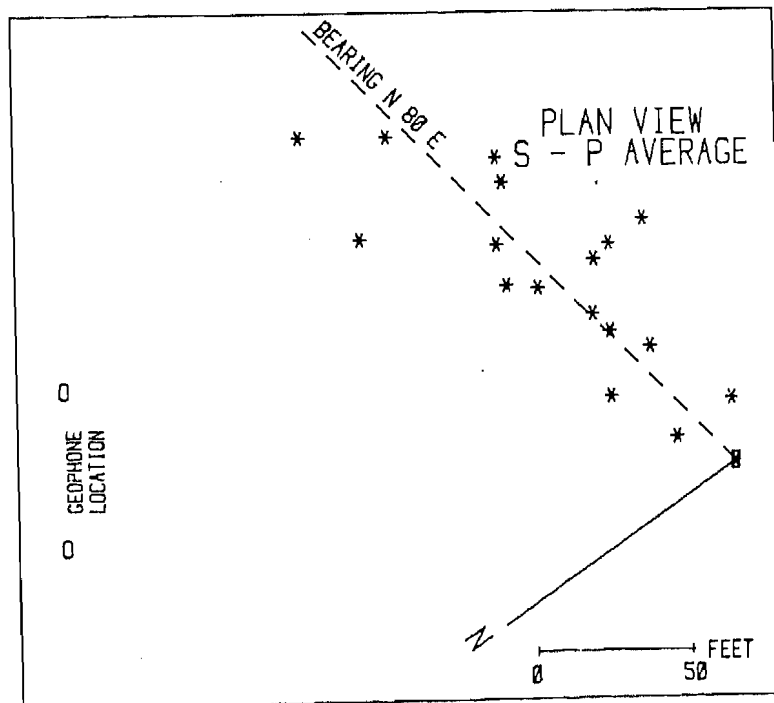


Figure 33. Source Locations Determined by Differences in S- and P-Wave Arrivals; Plan View.

at three locations. For eighteen signals, source locations were calculated from the data of each of the four geophone packages. The average of these four calculations is shown in the plan view in Fig. 33. The projected direction of the fracture is N 80° E. Figure 34 shows the vertical position of the calculated locations projected onto the N 80° E plane. In a different treatment of the data the average positions from the vector solution of each triaxial geophone package are plotted in Fig. 35. The fracture extends away from the wellbore at N53.5°E. Figure 36 is a plot of this calculated location projected on a vertical plane through the N53.5°E line.

The mineback, which began in September 1977, will continue throughout 1978. The proposed mineback route should intercept the fracture at the closest possible location and then follow the fracture back towards the well bore. The drift will be

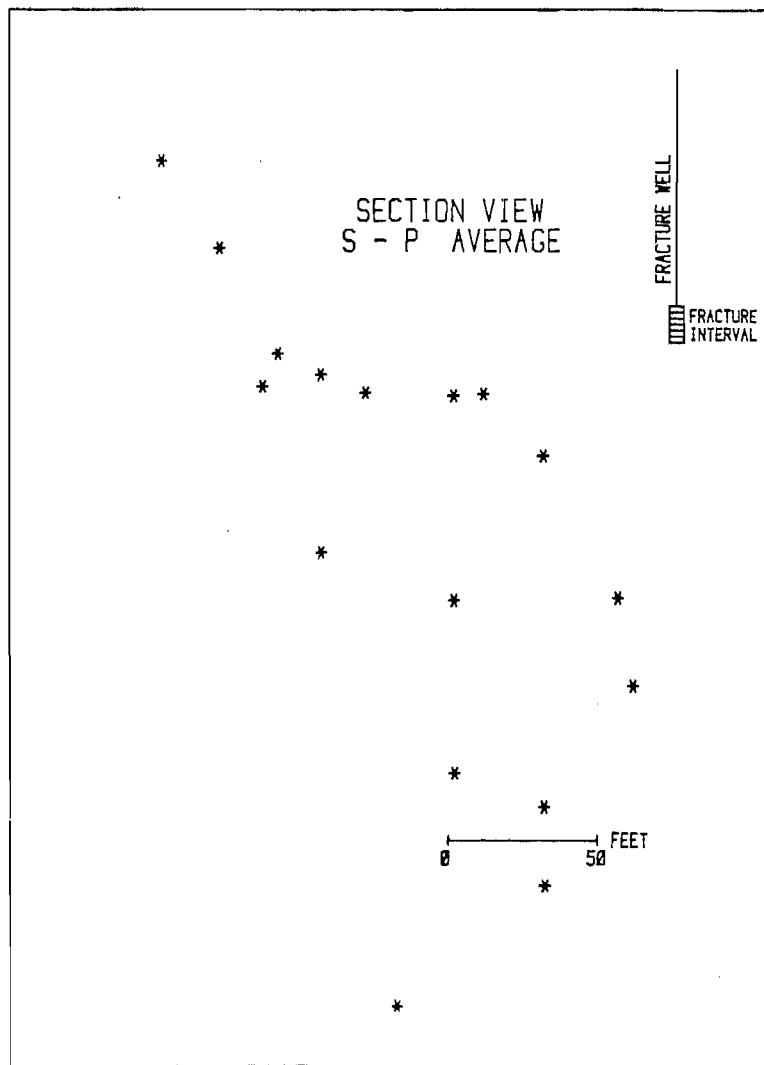


Figure 34. Source Locations Determined by Differences in S- and P-Wave Arrivals; Vertical Section Projected on N 80° E Plane.

cut just under the interface in order to obtain as much information as possible on the behavior of the fracture at the interface and to facilitate mining. Mining through the soft ash-fall tuff is considerably faster than mining through the welded tuff.

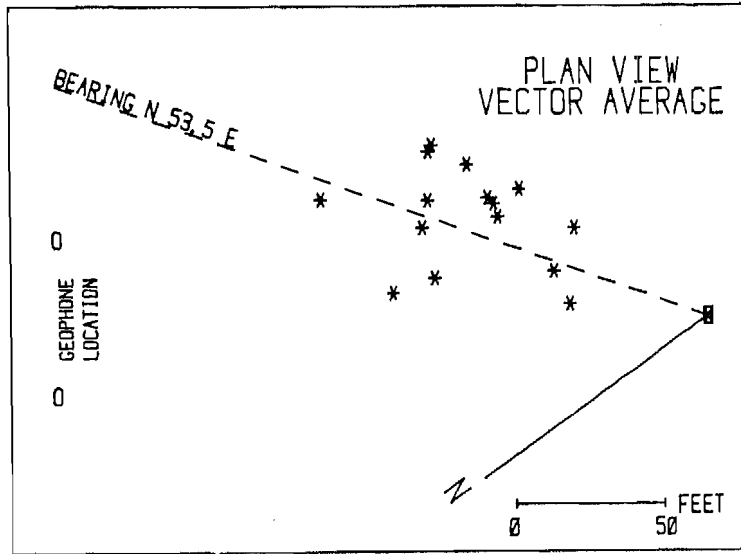


Figure 35. Source Locations Determined by Average of Vector Solutions for Each Triaxial Geophone Package; Plan View.

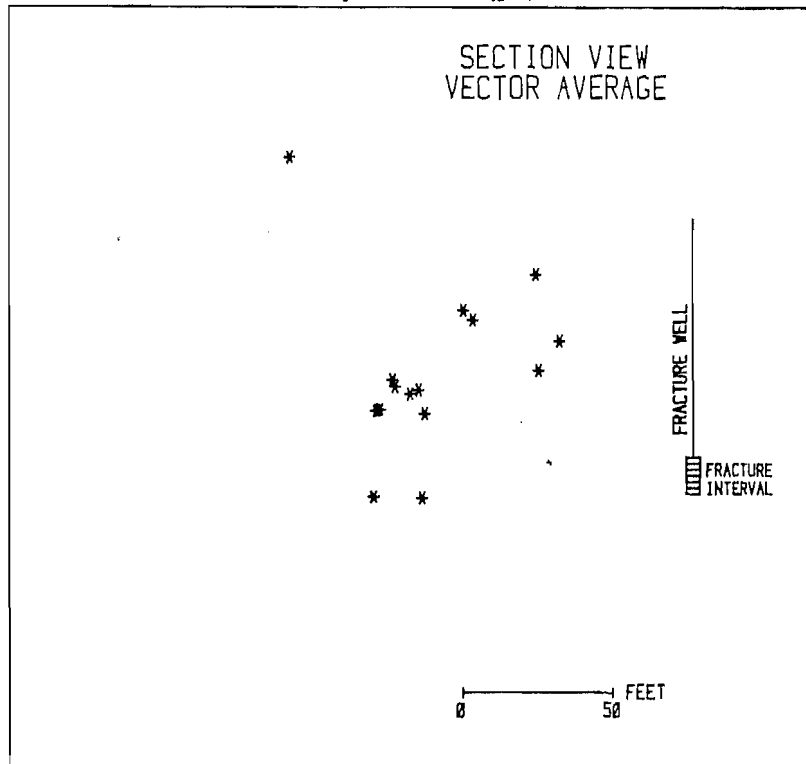


Figure 36. Source Locations Determined by Average of Vector Solutions for each Triaxial Geophone Package; Vertical Section Projected on N 53.5°E Plane.

## SUMMARY

An experiment has been designed and conducted which examines the behavior of hydraulic fractures created above and below a geologic formation interface. This report presents available data and discussion pertinent to the experiment after fracturing but prior to mineback operations. Mineback through the experimental region will allow direct observation of the behavior of the created fracture systems. The two data sets will then be combined at a later date to provide a better understanding of hydraulic fracturing.

The geology of the experimental region has been described in detail. The interface between an ash-fall tuff and a welded tuff was selected for the experiment and material properties from cores, logs, and rock samples have been detailed for the two formations. Particularly notable are significant differences in modulus ( $0.24 \times 10^6$  and  $3.8 \times 10^6$  psi), Poisson's ratio (0.312 and 0.238), porosity (45 and 13%), and density (1.8 and 2.4 gm/cc). The in situ stresses in the experimental region have been measured by hydraulic and overcore techniques.

The fractures have been designed by conventional techniques to be 50 ft high and 300 ft on a wing. The effects of material properties (modulus, Poisson's ratio, porosity, permeability), fluid loss coefficients, and fluid behavior on fracture growth have been parameterized to examine the effects that variations might produce. Rheological curves for the fracturing fluid, a dyed Class "A" cement, have been determined and have been fit to different fluid models.

The two hydraulic fractures were conducted in August and October, 1977. Pumping schedules, flow rates, well-head and bottomhole pressure were recorded and have been examined. The volume of the lower fracture in the ash-fall tuff was 9000 gal of green and black grout pumped in two stages; 5000 gal of blue grout was used in the upper, welded tuff interval. Pumping rates were 6 bbls/min and a water pad-and-flush was used in each instance. Acoustic signals were recorded during fracturing by triaxial geophone packages located in nearby boreholes; apparent signal source locations provide a clue as to fracture orientation. Mineback towards the fractures has been initiated.

Previous laboratory and modeling examinations of the behavior of a fracture at an interface does not allow a quantitative prediction of the fracture behavior in this field experiment. In fact, disparate conditions exist: a "well-bonded" interface, which would tend to allow fracture propagation, and a large difference in modulus which, according to fracture mechanics, would prevent a fracture from propagating from a lower to a higher modulus material. It is just these questions

that this experiment was designed to investigate.

#### ACKNOWLEDGMENTS

Sincere appreciation is given to Willian C. Vollendorf, other Sandia personnel, and the skilled G-Tunnel mining crew who conduct the tests, evaluations, and other operations at the Nevada Test Site. Thanks are also extended to Dowell personnel for conducting the two hydraulic fracture jobs. Robert W. Seavey of Sandia was responsible for the design, fielding and analysis of the acoustic instrumentation.

This project is supported by the Division of Oil, Gas, Shale and In Situ Technology, U. S. Department of Energy; Mr. Don C. Ward (Branch Chief), Jeff C. Smith and Alex B. Crawley manage the Enhanced Gas Recovery Program.

#### REFERENCES

1. L. D. Tyler and W. C. Vollendorf, "Physical Observations and Mapping of Cracks Resulting from Hydraulic Fracturing In Situ Stress Measurements," SPE 5542, Dallas, Texas, Sept. 28 - Oct. 1, 1975.
2. C. L. Schuster, "Natural Gas Massive Hydraulic Fracture Research and Advanced Technology Project Quarterly Report, November 1976 - January 1977," Sandia Laboratories Report, SAND77-0475, April 1977.
3. L. D. Tyler, W. C. Vollendorf, and D. A. Northrop, "In Situ Examination of Hydraulic Fractures," presented at Third ERDA Symposium for Enhanced Oil, Gas Recovery and Improved Drilling Methods, Aug. 30 - Sept. 1, 1977, Tulsa, Oklahoma.
4. C. L. Schuster and D. A. Northrop (Editors), "Natural Gas Massive Hydraulic Fracture Research and Advanced Technology Project Quarterly Report, February 1977 - April 1977," Sandia Laboratories Report, SAND77-1132, July 1977.
5. D. A. Northrop and C. L. Schuster (Editors), "Enhanced Gas Recovery Program, Second Annual Report, October 1976 - September 1977," Sandia Laboratories Report, SAND77-1992, April 1978.
6. P. L. Randolph, "Massive Stimulation Effort May Double U. S. Gas Supply," World Oil, October 1974 p. 132.
7. L. E. Elkins, "The Role of Massive Hydraulic Fracturing in Exploiting Very Tight Gas Deposits," and P. L. Randolph, "Natural Gas Production from a Tight Sandstone Reservoir in the Green River Basin of Southwestern Wyoming," Natural Gas From Unconventional Sources, National Academy of Sciences, FE-2271-1, 1976.
8. G. C. Howard and C. R. Fast, Hydraulic Fracturing, Society of Petroleum Engineers of AIME Monograph Series, 1970, Dallas, Texas.

9. A. A. Daneshy, "Hydraulic Fracture Propagation in Layered Formations," Soc. Petroleum Engineers Journal, February 1978, p. 33-41.
10. C. H. Elder, "Effects of Hydraulic Stimulation on Coalbeds and Associated Strata," R. I. 8260, U. S. Bureau of Mines, 1977.
11. M. E. Hanson, et. al. "LLL Gas Stimulation Program, Quarterly Progress Report, October through December, 1977," Lawrence Livermore Laboratory Report, UCRL-50036-77-4, January 1978.
12. E. R. Simonson, A. S. Abou-Sayed, and R. J. Clifton, "Containment of Massive Hydraulic Fractures," Soc. Petroleum Engineers Journal, February 1978, p. 27-32.
13. L. A. Rogers, E. R. Simonson, A. S. Abou-Sayed, and A. H. Jones, "Massive Hydraulic Fracture Containment Analysis Utilizing Rock Mechanics Considerations," Proceedings of the Massive Hydraulic Fracturing Symposium, University of Oklahoma, Norman, Oklahoma, February 28 - March 1, 1977.
14. T. S. Cook, and F. Erdogan, "Stresses in Bonded Materials with a Crack Perpendicular to the Interface," Inter. J. of Eng. Sci., Vol. 10, pp. 677-697, 1972.
15. F. Erdogan, and V. Biricikoglu, "Two Bonded Half Planes with a Crack Going through the Interface," Inter. J. of Eng. Sci., Vol. 11, pp. 745-766, 1973.
16. C. Atkinson, "On the Stress Intensity Factors Associated with Cracks Interacting with an Interface between Two Elastic Media," Inter. J. of Eng. Sci., Vol. 13, pp. 489-504, 1975.
17. R. K. Leverenz, "A Finite Element Stress Analysis of a Crack in a Bi-Material Plate," Inter. J. of Fracture Mechanics, Vol. 8, No. 3, pp. 311-324, Sept. 1972
18. D. B. Bogy, "On the Plane Elastostatic Problem of a Loaded Crack Terminating at a Material Interface," J. of Applied Mechanics, Vol. 38, pp. 911-918, Dec. 1971.
19. C. Atkinson, "Some Results on Crack Propagation in Media with Spatially Varying Elastic Moduli," Inter. J. of Fracture, Vol. 11, No. 4, pp. 619-628, August 1975.
20. S. E. Benzley and Z. E. Beisinger, "CHILES 2 - A Finite Element Computer Program that Calculates the Intensities of Linear Elastic Singularities in Isotropic and Orthotropic Materials," Sandia Laboratories Report, SAND77-1900, February 1978.
21. J. R. Ege and W. H. Lee, "Geologic Atlas of Ranier Mesa, Nevada Test Site, Nye County, Nevada," USGS Technical Letter, Ranier Mesa-13, 1971.
22. W. L. Ellis and J. R. Ege, "Determination of In Situ Stress in U12g Tunnel, Ranier Mesa, Nevada Test Site, Nevada," USGS Technical Letter, Area 12-37, 1971.

23. R. P. Snyder, "Electric and Caliper Logs as Lithologic Indicators in Volcanic Rocks, Nevada Test Site," in Nevada Test Site, Edwin B. Eckel (ed.), Geological Society of America, Boulder, Colorado, 1968.
24. V. E. Hooker, J. R. Aggson, and D. L. Bickel, "In Situ Determination of Stresses, Ranier Mesa, Nevada Test Site," United States Department of the Interior Bureau of Mines, August, 1971.
25. C. H. Miller, D. R. Miller, W. L. Ellis, and J. R. Ege, "Determination of In Situ Stress at U12e.18 Working Point, Ranier Mesa, Nevada Test Site," USGS Technical Letter, Area 12-42, Dec. 1975.
26. B. C. Haimson, J. Lacombe, A. H. Jones, and S. J. Green, "Deep Stress Measurements in Tuff at the Nevada Test Site," Proceedings of the Third Conference International Society of Rock Mechanics, Denver, Colorado, 1974, p. 557-562.
27. C. H. Miller, "A Method for Stress Determination in N, E, and T Tunnels, Nevada Test Site, by Hydraulic Fracturing, with a Comparison of Overcoring Methods," USGS Technical Letter, Area 12-43, May 1976.
28. M. K. Hubbert and D. G. Willis, "Mechanics of Hydraulic Fracturing," Petroleum Transactions, AIME, Vol. 210, 1957, p. 153-166.
29. R. O. Kehle, "The Determination of Tectonic Stresses Through Analysis of Hydraulic Well Fracturing," J. of Geophysical Research, Vol. 69, No. 2, Jan. 15, 1964.
30. L. Obert and W. I. Duvall, Rock Mechanics and the Design of Structures in Rock, John Wiley and Sons, Inc., New York, 1967.
31. B. Haimson and C. Fairhurst, "Initiation and Extension of Hydraulic Fractures in Rocks," Soc. of Petroleum Engineers J., Vol. 7, Sept. 1967, p. 310-318.
32. L. D. Tyler and W. C. Vollendorf, private communication, 1977.
33. T. K. Perkins and L. R. Kern, "Widths of Hydraulic Fractures," J. of Petroleum Technology, Vol. 13, Sept. 1961, pp. 937-949.
34. J. Geertsma and F. de Klerk, "A Rapid Method of Predicting Width and Extent of Hydraulically Induced Fractures," J. of Petroleum Technology, Vol. 21, Dec. 1969, pp. 1571-1581.
35. C. L. Schuster and D. A. Northrop (Editors), "Natural Gas Massive Hydraulic Fracture Research and Advanced Technology Project, Quarterly Report, October - December, 1977," Sandia Laboratories Report, SAND78-1172, June 1978.